HHS Public Access

Author manuscript

Cell Rep. Author manuscript; available in PMC 2019 November 20.

Published in final edited form as:

Cell Rep. 2019 November 12; 29(7): 2054–2066.e6. doi:10.1016/j.celrep.2019.10.027.

Glycosylation of Specific Notch EGF Repeats by O-Fut1 and Fringe Regulates Notch Signaling in *Drosophila*

Ashutosh Pandey[1,5], **Beth M. Harvey**[2,5,6], **Mario F. Lopez**[1], **Atsuko Ito**[3], **Robert S. Haltiwanger**[2,3,*], **Hamed Jafar-Nejad**[1,4,7,*]

[1]Department of Molecular and Human Genetics, Baylor College of Medicine, Houston, TX 77030, USA

[2]Department of Biochemistry and Cell Biology, Stony Brook University, Stony Brook, NY 11794, USA

[3]Complex Carbohydrate Research Center, University of Georgia, Athens, GA 30602, USA

[4]Program in Developmental Biology, Baylor College of Medicine, Houston, TX 77030, USA

[5]These authors contributed equally

[6]Present address: Department of Cell and Developmental Biology, University of Pennsylvania, Philadelphia, PA 19104, USA

[7]Lead Contact

SUMMARY

Fringe glycosyltransferases differentially modulate the binding of Notch receptors to Delta/DLL versus Serrate/Jagged ligands by adding GlcNAc to *O*-linked fucose on Notch epidermal growth factor-like (EGF) repeats. Although Notch has 22 *O*-fucosylation sites, the biologically relevant sites affecting Notch activity during animal development *in vivo* in the presence or absence of Fringe are not known. Using a variety of assays, we find important roles in *Drosophila* Notch signaling for GlcNAc-fucose-*O* glycans on three sites: EGF8, EGF9, and EGF12. *O*-Fucose monosaccharide on EGF12 (in the absence of Fringe) is essential for Delta-mediated lateral inhibition in embryos. However, wing vein development depends on the addition of GlcNAc to EGF8 and EGF12 by Fringe, with a minor contribution from EGF9. Fringe modifications of EGF8 and EGF12 together prevent Notch from *cis*-inhibiting Serrate, thereby promoting normal wing margin formation. Our work shows the combinatorial and context-dependent roles of GlcNAc-fucose-*O* glycans on these sites in *Drosophila* Notch-ligand interactions.

*Correspondence: rhalti@uga.edu (R.S.H.), hamedj@bcm.edu (H.J.-N.).

AUTHOR CONTRIBUTIONS

A.P., B.M.H., R.S.H., and H.J.-N. designed and conceived the project and interpreted the data. A.P. and B.M.H. performed the experiments. M.F.L. and A.I. contributed to the reagent preparations. A.P., B.M.H., R.S.H., and H.J.-N. wrote the manuscript.

DECLARATION OF INTERESTS

The authors declare no competing interests.

SUPPLEMENTAL INFORMATION

Supplemental Information can be found online at https://doi.org/10.1016/j.celrep.2019.10.027.

In Brief

POFUT1/O-Fut1 and Fringe glycosyltransferases regulate Notch signaling by adding fucose and GlcNAc, respectively, to Notch EGF repeats. Using *in vitro* and *in vivo* experiments, Pandey et al. define the critical target sites of these enzymes on *Drosophila* Notch and determine the distinct roles of each sugar in Notch-dependent processes.

Graphical Abstract

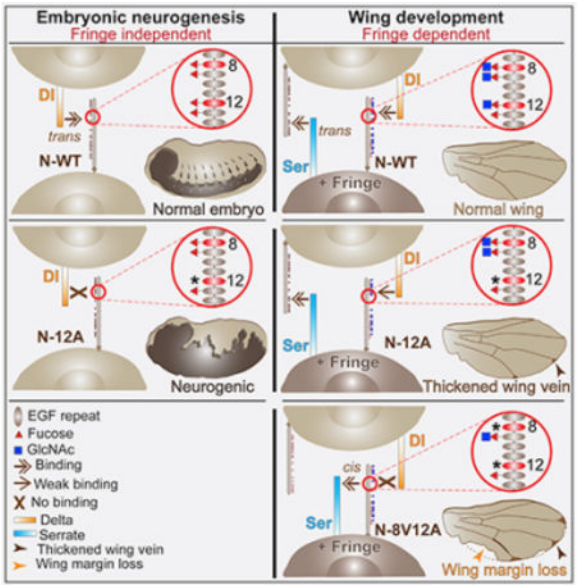

INTRODUCTION

Notch signaling is one of the evolutionary conserved signaling pathways required for development and tissue homeostasis in metazoans (Artavanis-Tsakonas and Muskavitch, 2010). Notch receptors and their canonical ligands from Delta (Dl)/DLL and Serrate (Ser)/Jagged (JAG) families are transmembrane proteins with multiple epidermal growth factor-like (EGF) repeats in their extracellular domains (Rebay et al., 1991). The interaction of Notch receptors with ligands from adjacent cells activates Notch signaling, or *trans*-activation (Bray, 2006). In addition, the interaction between Notch receptors and ligands from the same cell usually (but not always; Nandagopal et al., 2019) results in the inhibition of signaling, and these so-called *cis*-inhibitory interactions affect the outcome of Notch signaling in some contexts *in vivo* (Baek et al., 2018; Cordes et al., 2004; de Celis and Bray, 1997; Doherty et al., 1996; Geffers et al., 2007; Henrique et al., 1997; Jacobsen et al., 1998; Klein et al., 1997; Micchelli et al., 1997; Sprinzak et al., 2010). Given the broad roles that Notch signaling plays in animal development and human disease, understanding the molecular mechanisms that modulate the activity of this pathway in various contexts is of great interest (Mašek and Andersson, 2017; Siebel and Lendahl, 2017).

Most EGF repeats of Notch receptors harbor glycosylation sites for one or more forms of *O*-linked glycans, which play multiple roles in Notch signaling by affecting the folding,

trafficking, ligand binding, and/or cleavage of Notch receptors (Haltom and Jafar-Nejad, 2015; Stanley and Okajima, 2010; Takeuchi and Haltiwanger, 2014). One of the major forms of Notch *O*-glycosylation is *O*-fucosylation, which is the addition of an *O*-fucose (*O*-fuc) residue onto Notch EGF repeats by the enzyme protein *O*-fucosyltransferase 1 (POFUT1; O-Fut1 in flies) (Moloney et al., 2000b; Okajima and Irvine, 2002; Wang et al., 2001; Wang and Spellman, 1998). *O*-Fucosylation takes place between the second and third conserved cysteine residues on a serine or threonine in EGF repeats with a $C^2X_{4–5}(S/T)C^3$ consensus sequence (Shao et al., 2003). The loss of *O*-fucosylation results in embryonic lethality and phenotypes resembling the loss of Notch signaling in flies and mammals, demonstrating that *O*-fucosylation is critical for Notch signaling (Okajima and Irvine, 2002; Sasamura et al., 2003; Shi and Stanley, 2003).

An *N*-acetylglucosamine (GlcNAc) residue can be added to *O*-fuc on some EGF repeats by β1,3*N*-acetylglucosaminyltransferase enzymes of the Fringe (Fng) family (Brückner et al., 2000; Harvey et al., 2016; Kakuda and Haltiwanger, 2017; Moloney et al., 2000a). *Drosophila* has a single Fng protein encoded by *fng*, while mammals have three homologs: Lunatic Fng (LFNG), Manic Fng (MFNG), and Radical Fng (RFNG) (Cohen et al., 1997; Irvine and Wieschaus, 1994; Johnston et al., 1997). The loss of *fng* in flies and of *Lfng* in mice recapitulate some but not all of the phenotypes associated with the loss of Notch signaling (Correia et al., 2003; Evrard et al., 1998; Irvine and Wieschaus, 1994; Zhang and Gridley, 1998). The enzymatic activity of Fng proteins on Notch receptors differentially regulates the activation of Notch by Dl/DLL versus Ser/JAG ligands (Brückner et al., 2000; Hicks et al., 2000; Moloney et al., 2000a; Panin et al., 1997). GlcNAcylation of the fly Notch by Fng enhances Dl-Notch binding and decreases Ser-Notch binding (Brückner et al., 2000; Xu et al., 2007). Therefore, GlcNAc residues added to one or more of the many Notch EGF repeats that have an *O*-fucosylation site must mediate the effects of Fng proteins on Notch signaling.

Biochemical and cell-based assays have made important progress toward the identification of those Notch EGF repeats whose glycosylation by POFUT1/O-Fut1 and Fng proteins can modulate Notch binding and activation by Dl/DLL and Ser/JAG ligands (Kakuda and Haltiwanger, 2017; Xu et al., 2005). However, the use of soluble forms of Notch and ligands in many such assays does not provide sufficient information to distinguish the effects of a given carbohydrate residue on *trans*- versus *cis*-interaction of Notch with ligands. Moreover, the overexpression of full-length Notch, ligand, and Fng proteins in cell culture assays may mask the effects of glycosylation on signaling at the endogenous levels of these proteins. Based on transgenic overexpression of the full-length fly Notch with mutations in individual *O*-fucosylation sites, a previous study concluded that Notch with an *O*-fuc site mutation in EGF12 is able to restore the Dl-mediated embryonic neurogenesis in *Notch* null embryos (Lei et al., 2003). However, it remains to be seen whether this is the case when Notch is expressed at endogenous levels and whether this glycan acts together with *O*-fuc monosaccharides on other Notch EGF repeats. A knockin allele of the mouse *Notch1* with an EGF12 *O*-fuc site mutation (*Notch1[12f]*) behaves as a hypomorphic allele (Ge and Stanley, 2008). Analysis of *Notch1[12f/12f]* thymocytes indicated that the *O*-fuc glycan on EGF12 is required for optimal DLL-mediated activation of NOTCH1 in these cells. However, whether this effect is mediated by GlcNAc, fuc, or both is not known.

Here, we report our studies on the contribution of Fng-modified *O*-fuc glycans on specific Notch EGF repeats to Notch signaling and the Fng effect in *Drosophila*. Quantitative and saturable *in vitro* binding assays indicated a potential role for GlcNAcylation of *O*-fuc on Notch EGF8, EGF9, and EGF12 in mediating the effects of Fng on Notch-ligand binding. *In vivo* structure function and genetic interaction experiments, combined with cell-based aggregation assays, revealed both distinct and redundant roles for individual GlcNAc and/or fuc residues on EGF8, EGF9, and EGF12 in regulating the *cis*- and *trans*-interactions of Notch with Dl and Ser ligands. Our data determine the functional importance of specific carbohydrate residues attached to Notch in regulating distinct Notch-ligand interaction modalities and establish the Notch EGF repeats that mediate the effects of Fng in fly Notch signaling.

RESULTS

A Modified Notch-Ligand Binding Assay Recapitulates Fng *In Vivo* Effects and Reveals Differential Mechanistic Effects on Notch Binding to Dl and Ser

To investigate the mechanisms of how Fng modulates Notch-ligand binding, we modified a mammalian cell-based binding assay so that it could be used for *Drosophila* S2 cells (Kakuda and Haltiwanger, 2017). To simply and directly examine ligand binding, we used a Notch-CD2 (N-CD2) hybrid receptor that expresses EGF repeats 1–36 from the extracellular domain of fly Notch fused with the CD2 transmembrane protein (Figures 1A and S1A) (Brückner et al., 2000; Yamamoto et al., 2012). Ligand proteins used for binding assays were purified from the media of S2 cell lines stably expressing the extracellular domains of Dl and Ser with C-terminal Myc-6xHis tags (Figures 1A and S1B). Before testing ligand binding, we confirmed the cell surface expression of N-CD2 using flow cytometry and also observed that it was not affected by Fng co-expression (Figure S1C). For these assays, it is advantageous that S2 cells do not exhibit endogenous Fng activity (Moloney et al., 2000a), and mass spectrometry on Notch isolated from S2 cells did not detect GlcNAc on *O*-fucosylated EGF repeats (Harvey et al., 2016). We then tested the increasing ratios of Fng co-transfected with N-CD2 into S2 cells incubated with ligand to examine the effect of Fng expression on the binding of N-CD2 to Dl and Ser. We observed that increasing Fng co-expression increases Dl binding (Figures 1B and S1D) but decreases Ser binding (Figures 1C and S1E). In both cases, the Fng effects were observed at very low Fringe:Notch ratios. To confirm that the effects on ligand binding in our assays were in fact due to Fng glycosyltransferase activity, we mutated the DXD motif to generate an enzymatically inactive Fng (DEE Fringe) (Moloney et al., 2000a). Western blots of transfected cell lysates showed that the enzymatically inactive Fng is expressed at levels similar to those of wild-type (WT) Fng (Figure S1F). We observed that while co-expression of N-CD2 with Fng increased Dl binding and decreased Ser binding, co-expression with DEE Fng showed binding similar to that in the absence of Fng, demonstrating that Fng glycosyltransferase activity on N-CD2 specifically affects ligand binding (Figure S1G).

To examine the differential effects of Fng on Notch-ligand binding in more detail, we analyzed the concentration dependence of ligand binding. Dl bound minimally to N-CD2 cells in the absence of Fng, with only moderate increases in binding upon increased Dl

concentrations (Figure 1D, −Fringe). The Notch-Dl binding did not reach saturation in the absence of Fng and therefore precluded the estimation of either Bmax or Kd. However, Fng greatly increased Dl binding, such that Dl binding was saturable, which allowed for the determination of estimated Bmax and Kd values (Figure 1D, +Fringe). These data suggest that Fng dramatically decreases the Kd for Notch binding to Dl. In contrast, Ser binding to N-CD2 was decreased in the presence of Fng compared to the absence of Fng (Figure 1E). Ser binding was also saturable. We found that Fng reduced both the Bmax and the Kd of Notch binding to Ser (Figure 1E). These observations indicate that Fng mostly affects the affinity (Kd) of Notch for Dl, while it alters both the number of binding sites (Bmax) and the affinity between Ser and Notch. These data reveal distinct mechanisms for how Fng mediates its differential effects on Notch interactions with Dl and Ser ligands.

Cell-Based Assays Suggest That *O*-Fucosylation at Notch EGF8, EGF9, and EGF12 Are Important for Fng to Modulate Notch-Ligand Binding

To gain further insight into the roles of specific Fng-elongated *O*-fuc sites of Notch on modulating ligand binding, we performed site-directed mutagenesis of 19 of the 22 *O*-fuc sites of fly Notch. To abolish *O*-fucosylation without dramatically changing the amino acid size, we introduced threonine-to-valine (T-to-V) and serine-to-alanine (S-to-A) mutations and named the mutant EGF repeats accordingly (e.g., EGF8V, EGF9V, EGF12A). Mutants of EGF2, EGF31, and EGF32 *O*-fuc sites were not generated since they are not efficiently modified by Fng (Figure 1A; Harvey et al., 2016). Although *O*-fuc on EGF13 and EGF26 was also poorly modified by Fng (Harvey et al., 2016), these sites were mutated due to their proximity to the ligand-binding domain (Rebay et al., 1991) and location within the *Abruptex* domain (Kelley et al., 1987), respectively (Figure 1A). We performed flow cytometry and western blotting to show that each N-CD2 *O*-fuc site mutant was expressed on the cell surface and at expected molecular weights (Figures S2A and S2B). We then analyzed the binding of each N-CD2 *O*-fuc site mutant to Dl and Ser in the presence and absence of Fng (Figures S2C and S2D; Table S2). Mutation in *O*-fuc sites of EGF8, EGF9, and EGF12 mediated distinct effects on Dl and Ser binding (Figure 2). These *O*-fuc site mutants were tested in binding assays with varied levels of Fng expression (Figure 2A). Mutating the *O*-fuc site on EGF9 slightly reduced Fng-dependent Dl binding, while mutating the *O*-fuc sites at EGF8 and EGF12 had larger effects (Figure 2A). N-CD2 with mutations in both EGF8 and EGF9 (8V9V) showed an additive effect, and N-CD2 with mutations in both EGF8 and EGF12 (8V12A) was completely unable to bind Dl with any amount of Fng (Figure 2A). Although the 8V, 8V9V, and 8V12A mutants showed slightly reduced cell surface expression (Figure S2A), this was not sufficient to account for the effect seen on ligand binding. Additional binding assays at a single Fringe:Notch ratio corroborated these results (Figures 2B and S2C). These data suggest that Fng modification of *O*-fuc on EGF8, EGF9, and EGF12 contributes to Dl binding, and modification of *O*-fuc on EGF8 and EGF12 is critical for Fng enhancement of Notch-Dl binding.

Different effects on Notch-Ser binding were observed upon using varying levels of Fringe:Notch ratios with the EGF8, EGF9, and EGF12 *O*-fuc site mutants (Figure 2C). Most striking was the effect of the EGF12 mutant, which showed enhanced Ser binding in the absence of Fng, suggesting an inhibitory role of *O*-fuc at this site (Figures 2C and 2D). The

mutations at EGF8 and EGF9 had reduced Ser binding in the absence of Fng, suggesting that *O*-fuc at these sites contributes to Ser interactions with Notch, and mutation of both EGF8 and EGF9 (8V9V) almost eliminated binding (Figures 2C and 2D). Fng co-expression with the EGF9 and EGF12 mutants still reduced Ser binding, suggesting that *O*-fuc on EGF9 and EGF12 is not essential for the Fng effects on Ser (Figures 2C and 2D). All of the mutants containing an EGF8 *O*-fuc site mutation (8V, 8V9V, 8V12A) showed no significant reduction in Ser binding with Fng co-expression, suggesting that Fng modification of the *O*-fuc on EGF8 plays a major role in inhibiting Ser binding (Figures 2C, 2D, and S2D). These results reveal distinct roles of the *O*-fuc modifications on EGF8, EGF9, and EGF12 for Fng to modulate Notch binding to Dl and Ser.

O-Fucosylation Site Mutations in Individual Notch EGF Repeats or Their Pairwise Combinations Do Not Affect the Notch Cell Surface Levels in *Drosophila*

Based on our cell-based data, we sought to perform an *in vivo* functional assessment of the GlcNAc-fuc-*O* glycans on EGF8, EGF9, and EGF12 of fly Notch. We used a previously established gap-repair mutagenesis strategy (Leonardi et al., 2011; Leonardi and Jafar-Nejad, 2014) to generate *Notch* genomic transgenes with T-to-V or S-to-A mutations that prevent *O*-fucosylation in EGF8, EGF9, or EGF 12 (*N[gt-8V], N[gt-9V],* and *N[gt-12A],* respectively) and in their pairwise combinations (*N[gt-8V9V], N [gt-8V12A],* and *N[gt-9V12A]*). Notch EGF5 shows a high level of *O*-fucosylation and GlcNAcylation (Figure 1A; Harvey et al., 2016) but does not show altered cell surface levels or ligand binding *in vitro* upon the loss of the GlcNAc-fuc-*O* glycan (Figure S2). Therefore, we also generated *N[gt-5V]* as a control for the *in vivo* studies.

Our S2 cell-based assays indicate that single *O*-fuc site mutations do not dramatically impair the surface expression of the Notch-CD2 hybrid protein (Figures S2A and S2B). However, the T-to-V and/or S-to-A mutations may affect the folding and cell surface trafficking of the full-length Notch in fly tissues independently of its glycosylation. Therefore, before performing functional studies, we examined the cell surface levels of mutant Notch proteins *in vivo*, as reported previously (Leonardi et al., 2011). Since *N[54I9]* is a protein null allele, *N[54I9]* homozygous clones do not show Notch extracellular domain (NECD) staining (Figures S3A–A“; Leonardi et al., 2011). Comparison of the relative signal intensities revealed no significant change in the cell surface level of any of the examined mutant Notch proteins compared to the WT Notch from *N[gt-wt]* (Figures S3B–S3J). We conclude that the loss of *O*-fucosylation from these Notch EGF repeats does not affect the cell surface level of Notch *in vivo*.

Loss of *O*-Fucosylation of Notch EGF12 Impairs Dl-Notch Signaling during *Drosophila* Embryonic Neurogenesis

Having assessed the Notch cell surface level upon mutating the Fng-modified *O*-fucosylation sites on the selected Notch EGF repeats, we examined their effect on Notch signaling *in vivo*. Fly *Notch* is an X-linked gene, and hemizygous males of *Notch* null alleles show embryonic lethality (Artavanis-Tsakonas et al., 1983). The lethality of hemizygous males (*N[−]/Y*) can be rescued by the addition of one copy of the WT *N[gt-wt]* (Figure 3A) (Leonardi et al., 2011). To examine whether mutation in the *O*-fuc sites of the

selected Notch EGF repeats (8V, 9V, 12A, 8V9V, 8V12A, and 9V12A) can rescue *N[−]/Y* lethality, we compared the survival of *N[−]/Y* males harboring one copy of mutant *Notch* transgenes with those harboring one copy of *N[gt-wt]*. The addition of one copy of *N[gt-5V]* and *N[gt-8V]* fully rescued the lethality of *N[−]/Y* males (Figure 3A). However, *N[gt-9V]* and *N [gt-8V9V]* showed a partial rescue compared to control animals (Figure 3A; 77% and 73%, respectively). Moreover, *N[gt-12A], N[gt-8V12A],* and *N[gt-9V12A]* did not rescue the *N[−]/Y* male lethality at all (Figure 3A). These data suggest an essential role for the *O*-fuc monosaccharide modification on Notch EGF12 and a minor but significant role for the *O*-fuc monosaccharide modification on EGF9 during fly development.

N[−]/Y embryos show a fully penetrant neurogenic phenotype (Figures 3C and C') due to impaired lateral inhibition, which is mediated by Dl-Notch signaling during *Drosophila* neurogenesis (Heitzler and Simpson, 1991). Of note, Notch signaling does not depend on *fng* at this stage, as *fng* mutant animals do not exhibit a neurogenic phenotype (Haines and Irvine, 2003). We examined the ability of these Notch transgenes to rescue the *N[−]/Y* neurogenic phenotype in embryos by performing ELAV staining, which marks a neuron-specific nuclear protein (Robinow and White, 1991). A full rescue of the neurogenic phenotype in *N[−]/Y* male embryos was observed upon the addition of a copy of *N[gt-wt], N[gt-5V],* or *N[gt-8V]* (Figures 3D–3F'). The addition of one copy of *N [gt-9V]* or *N[gt-8V9V]* showed a partial rescue of the neurogenic phenotype, in agreement with the partial rescue of lethality by these transgenes (Figures 3G–H' and 3J–3K'; 82% and 80% rescue, respectively). However, the addition of one copy of *N[gt-12A], N[gt-8V12A],* or *N[gt-9V12A]* did not show any rescue of the neurogenic phenotype in *N[−]/Y* male embryos (Figures 3I and 3I' and 3L–3M'). These data indicate the essential contribution of an *O*-fuc monosaccharide modification on Notch EGF12 and a partial role for an *O*-fuc monosaccharide modification on EGF9 in embryonic neurogenesis, likely via the regulation of Dl-mediated Notch signaling.

As mentioned above, Fng does not play a role in Dl-Notch-mediated lateral inhibition during embryonic neurogenesis (Haines and Irvine, 2003; Ishio et al., 2015). Therefore, the effects of *O*-fuc site mutations in EGF9 and EGF12 are likely due to the loss of *O*-linked fuc monosaccharide itself. However, it is possible that the mutations (T-to-V in EGF9 and S-to-A in EGF12) could alter the configuration of these EGF repeats due to the amino acid change and thus affect Notch signaling independently of the *O*-fuc linked to these sites, as previously shown for Cripto (Shi et al., 2007). Therefore, to determine whether the presence of *O*-fuc on these EGF repeats is specifically important for Dl-Notch signaling, we generated a threonine-to-serine mutation in EGF9 (9S) and a serine-to-threonine mutation in EGF12 (12T). These mutations will still allow for *O*-fucosylation of EGF9 and EGF12, although they change the hydroxy-amino acid. Mosaic analysis with a repressible cell marker (MARCM) clonal analysis showed that the 9S and 12T mutations did not affect the cell surface level of Notch (Figures S4A–S4C). Notably, both transgenes fully rescued the lethality and neurogenic phenotype in *N [−]/Y* males (Figures S4D–S4F'). These observations indicate that the *O*-fuc monosaccharide on Notch EGF12 (and to some extent the one on EGF9) is required for embryonic neurogenesis.

Fng Modification of EGF8 and EGF12 Plays a Major Role in Dl-Notch Signaling during Wing Vein Formation

Dl-Notch signaling in *Drosophila* embryonic neurogenesis is independent of Fng (Haines and Irvine, 2003; Ishio et al., 2015). Therefore, to examine the role of GlcNAc added to *O*-fucosylated Notch EGF repeats by Fng, we analyzed the *O*-fuc mutant *Notch* transgenes in two additional contexts in which Fng plays important roles: wing vein development and wing margin development (Correia et al., 2003). Fly wing vein development is primarily regulated by Dl-Notch signaling (de Celis et al., 1997; de Celis and Bray, 2000; Huppert et al., 1997), with a minor contribution from Ser-Notch signaling, which is only revealed when both ligands are mutated (Zeng et al., 1998). Adult wings from *Notch* heterozygous females (*N[+/−]*) show a fully penetrant wing vein-thickening phenotype (Figures 4A and 4J). The addition of one copy of *N[gt-wt]* rescues this phenotype (Figures 4B and 4J; Leonardi et al., 2011). Similarly, the addition of one copy of *N[gt-5V]* or *N[gt-8V]* fully rescued this phenotype (Figures 4C, 4D, and 4J). The addition of one copy of *N[gt-9V], N [gt-12A],* or *N[gt-9V12A]* partially rescued the phenotype in all *N[+/−]* flies (Figures 4E, 4F, 4I, and 4J), suggesting that the Fng modification of *O*-fuc on EGF9 and EGF12 contributes to Dl-mediated Notch signaling during normal wing vein development. In contrast, the addition of one copy of *N[gt-8V9V]* only showed a partial rescue in 22% of the animals and no rescue in the remaining 78% (Figures 4G and 4J). *N[gt-8V12A]* did not rescue the wing vein-thickening phenotype in any of the *N[+/−]* flies (Figures 4H and 4J). These data are in agreement with our *in vitro* assays (Figure 2B) and indicate that GlcNAc-fuc-*O* on EGF8, EGF9, and EGF12 contribute to the modulation of Dl-Notch signaling by Fng during wing vein development. The data also suggest that the glycans on EGF8 and EGF12 are more important than the glycan on EGF9 for this process.

Thus far, our data indicate that the impact of EGF12 *O*-fuc site mutation on embryonic neurogenesis (−Fringe; Figure 3) is dramatically different from its impact on wing vein development (+Fringe; Figure 4). To test whether Fng modification of EGF8 and EGF9 underlies this difference, we examined whether modulating the *fng* gene dosage affects the ability of *N[gt12A], N[gt-8V12A],* or *N[gt-9V12A]* transgenes to rescue the wing vein-thickening phenotype in *N[+/−]* flies. As shown in Figure 4J, adding one genomic copy of *fng* improved the ability of all three transgenes in rescuing the *N[+/−]* wing vein phenotype. Moreover, removing one copy of *fng* decreased the functionality of *N[gt12A]* and *N[gt-9V12A]* transgenes in this assay (Figure 4J). Note that *N[gt-8V12A]* did not show any rescue of this phenotype in an *fng[+/+]* or *fng[+/−]* background (Figure 4J). Adding or removing one copy of *fng* in a WT background does not have any wing vein phenotypes by itself (Figure 4J). These observations support the notion that the addition of GlcNAc to EGF8 and EGF9 partially masks the effects of the loss of the *O*-fucose glycan from EGF12.

We next decided to more directly assess the contribution of each sugar (unmodified *O*-fuc versus GlcNAc-extended *O*-fuc) on these EGF repeats to Dl-Notch interactions. We could not accurately measure Dl-Notch binding in the absence of Fng using our flow cytometric binding assays because the level of soluble Dl-Myc-6xHis binding was too low and saturation was never obtained (Figure 1D). Therefore, we used a well-established S2 cell-based aggregation assay to reveal the effect of *O*-fuc site mutations in the above-mentioned

EGF repeats on Notch-ligand binding in the presence and absence of Fng (Fehon et al., 1990; Lee et al., 2017; Pandey and Jafar-Nejad, 2018).

We performed aggregation assays between stable S2-Dl cells and S2 cells transiently transfected with inducible plasmids expressing full-length WT Notch (S2-N-WT) or mutated Notch (S2-N-12A, S2-N-8V, or S2-N-8V12A), with or without co-transfection of an Fng-expression construct. Untransfected S2 cells, which do not express Notch and Dl (Fehon et al., 1990), were used as experimental controls. As reported previously, mixing S2-Dl cells with S2 cells transfected with N-WT resulted in the formation of a number of aggregates (Figure 5A; Fehon et al., 1990; Lee et al., 2017). In the absence of Fng, we observed a significant decrease (>50%) in the number of aggregates between S2-Dl and S2-N-12A compared to controls (Figures 5A and 5B). In contrast, an *O*-fuc mutation in EGF8 did not affect the aggregation of S2-N-8V cells with S2-Dl cells (Figure 5C). Moreover, S2-N-8V12A cells, which express Notch molecules with EGF8 and EGF12 mutations, showed the same level of decrease in aggregation with S2-Dl as the single mutant S2-N-12A cells (Figure 5D). These observations indicate that in the absence of Fng, *O*-fuc on EGF12 plays a major role in promoting Dl-Notch interactions and that *O*-fuc on EGF8 cannot compensate for the loss of *O*-fuc from EGF12.

Upon co-expression of Fng, both S2-N-WT and S2-N-12A cells showed a significant increase in the number of aggregates with S2-Dl cells (Figures 5A and 5B), suggesting that the addition of GlcNAc to ≥1 Notch EGF repeats other than EGF12 can at least partially compensate for the decrease in Dl-Notch interaction caused by the *O*-fuc mutation in EGF12. However, Fng overexpression failed to significantly increase the number of aggregates between S2-N-8V12A and S2-Dl cells, although a weak trend toward increased aggregation was observed (Figure 5D). Fng overexpression also significantly enhanced the number of aggregates between S2-N-8V and S2-Dl cells (Figure 5C). These results provide strong evidence that the Fng-mediated enhancement of Dl-Notch-12A interaction is primarily mediated by GlcNAcylation of *O*-fucosylated EGF8. They are also consistent with our flow cytometric binding assay (Figures 2A and 2B).

Fng Prevents Notch from *cis*-Inhibiting Ser by Adding GlcNAc to EGF Repeats 8 and 12

Along with wing vein thickening, *N[+/−]* females also show a mild wing margin loss phenotype (Figures 4A and 6A; ~40% penetrant). Although both Dl and Ser ligands are involved in wing margin formation, this process is more sensitive to Ser-Notch signaling (de Celis and Bray, 1997; Doherty et al., 1996; LeBon et al., 2014). Moreover, Fng plays a key role in wing margin development (Irvine and Wieschaus, 1994). The addition of one copy of *N[gt-wt]* and most mutant transgenes fully rescued the wing margin loss phenotype of *N[+/−]* females (Figures 4B–4G, 4J, and 6A). Unexpectedly, *N[gt-8V12A]* not only failed to rescue the wing margin phenotype of *N[+/−]* females but also enhanced its penetrance (Figure 6A; 60% penetrant) and severity (Figure 4H). These observations suggest that GlcNAc-fuc-*O* glycans on EGF8 and EGF12 are redundantly required for wing margin formation.

In fly wing discs, Notch can *cis*-inhibit Ser, although the role of Fng in this process has not been examined (Becam et al., 2010). Accordingly, we hypothesized that the enhancement of

the *N[+/−]* wing margin phenotype by *N[gt-8V12A]* may be due to the enhanced *cis*-inhibition of Ser by N-8V12A. To examine the Ser-Notch *cis*-binding, we performed aggregation assays between stable S2-Notch (S2-N) cells (without Fng expression) and S2 cells transiently transfected with an Ser expression vector alone (S2-Ser) or co-transfected with WT or mutant Notch (S2-Ser-N or S2-Ser-N8V12A). The relative aggregation between S2-N and S2-Ser cells in the presence and absence of *cis*-Notch was used as an indication of the degree of the *cis*-inhibitory effect of Notch on Ser. For example, if the number of aggregates between S2-N and S2-Ser-N cells is 30% of the number of aggregates between S2-N and S2-Ser cells (i.e., relative aggregation 30%), we would conclude that *cis*-Notch was able to inhibit the interaction between Ser and *trans*-Notch by 70%. In the absence of Fng, the number of aggregates between S2-N and S2-Ser-N cells was significantly decreased compared to that between S2-N and S2-Ser cells (Figures 6B and 6C), indicating the inhibitory effect of *cis*-Notch on Ser. Co-expression of Fng in the S2-Ser-N cells resulted in a significant increase in the number of aggregates with S2-N cells compared to the number of aggregates between S2-N and S2-Ser-N cells in the absence of Fng (Figures 6B and 6C). Of note, the co-expression of Fng in S2-Ser cells (without Notch co-expression) did not affect the aggregation of these cells with S2-N cells (Figures 6B and 6C). Moreover, as expected, the overexpression of Fng in S2-N cells decreased the aggregation of these cells with S2-Ser^{Tom} cells, which stably express a Tomato-tagged version of Ser (Figure S5; Fleming et al., 2013). These observations indicate that the increased aggregation between S2-Ser-N and S2-N cells upon Fng overexpression can be explained by the reduction of Ser-Notch *cis*-binding by Fng and the consequent enhancement in Ser-Notch *trans*-binding, not by a direct effect of Fng on Ser-Notch *trans*-binding or on the Ser protein itself.

Similar to the WT Notch, the co-expression of N-8V12A with Ser significantly decreased the number of aggregates with S2-N cells, suggesting that N8V12A is still capable of mediating *cis*-inhibition (Figures 6B and 6C). However, co-expression of Fng was not able to relieve the *cis*-inhibitory effect of N8V12A on Ser (Figures 6B and 6C). This is consistent with the data in Figure 2D, in which Fng does not affect the binding between N-CD2–8V12A and Ser. These data suggest that the loss of GlcNAc-fuc-*O* from both EGF8 and EGF12 enhances the Ser-Notch *cis*-binding and leads to *cis*-inhibition of Ser by Notch, even in the presence of Fng.

In agreement with these cell-based aggregation assays, providing a genomic copy of *Ser* but not *Dl* significantly decreased the penetrance and severity of the wing margin loss phenotype in *N[+/−]; N[gt-8V12A/+]* animals (Figures 7A–7D and 7G). In addition, in an *N[+/+]* background, two copies of *N[gt-8V12A/+]* resulted in wing margin loss in ~23% of the animals (Figures 7E and 7G). Again, an extra copy of Ser significantly reduced the penetrance of this phenotype (Figures 7F and 7G; 9% penetrant). Together with our *in vitro* and cell culture observations, these data indicate that Fng modification of *O*-fuc on EGF8 and EGF12 prevents Notch from *cis*-inhibiting Ser and thereby allows normal wing margin development in *Drosophila*.

DISCUSSION

Fng proteins play important roles in Notch signaling by adding GlcNAc residues to *O*-fucosylated EGF repeats on Notch receptors (Harvey and Haltiwanger, 2018; Varshney and Stanley, 2018). Since Fng proteins differentially regulate the binding and response of Notch to the Dl/DLL versus Ser/JAG ligands, identification of the Notch EGF repeat(s) whose glycosylation mediates the Fng effects can provide important insight into Notch-ligand interactions. For many years, EGF11 and EGF12 were thought to make up the ligand-binding domain of Notch receptors (de Celis et al., 1993; Rebay et al., 1991), although it was suggested that additional EGF repeats may also contribute to ligand binding (Lawrence et al., 2000). More recent biochemical, structural, mammalian cell culture, and fly genetic studies have provided evidence for a more extended ligand-binding domain spanning EGF8–EGF12 (Figure 1A; Andrawes et al., 2013; Kakuda and Haltiwanger, 2017; Luca et al., 2017; Yamamoto et al., 2012). Using *in vitro* and *in vivo* analyses, we report here that GlcNAc-fuc-*O* glycans on EGF8, EGF9, and EGF12 play important roles in the regulation of fly Notch signaling. While the importance of Fng modifications of *O*-fuc on EGF8 and EGF12 is consistent with recent work on mouse NOTCH1, we cannot exclude the potential contribution of other EGF repeats to the Fng effect in flies, as recently suggested for mouse NOTCH1 based on studies in a mammalian cell line (Kakuda and Haltiwanger, 2017). Nevertheless, our data demonstrate that glycosylation of the extended ligand-binding domain of Notch by O-Fut1 and Fng plays critical roles in fly Notch signaling.

Previous studies have provided strong evidence that the inhibitory effect of mammalian Fng proteins on JAG1-mediated NOTCH1 signaling is not mediated at the level of JAG1-NOTCH1 binding (Hicks et al., 2000; Kakuda and Haltiwanger, 2017; Taylor et al., 2014; Yang et al., 2005). In fact, so far, biochemical and cell-based assays indicate that Fng modifications enhance NOTCH1-JAG1 interactions (Kakuda and Haltiwanger, 2017; Taylor et al., 2014). This suggests that the negative regulation of JAG1-NOTCH1 signaling by Fng occurs at a step after the initial ligand binding (Kakuda and Haltiwanger, 2017). In contrast, our data indicate that *Drosophila* Fng modifications affect the binding of Notch with Ser in a manner that is consistent with its effect on signaling, as evidenced by decreased Kd (affinity) and Bmax (number of binding sites) (Figure 1E). The reduction of Bmax suggests that Fng modifications could affect Notch conformation or promote Notch dimerization/multimerization. Regardless of the mechanism, this is in agreement with previous reports that showed that the co-expression of Fng with Notch in S2 cells impairs the binding of Notch to Ser (Okajima et al., 2003; Xu et al., 2007; Yamamoto et al., 2012). We conclude that despite the similarity between the *in vivo* roles of fly and mammalian Fng proteins in the regulation of Notch signaling, some differences are likely to exist in the molecular mechanisms through which Fng proteins regulate *Drosophila* versus mammalian Notch signaling.

The overexpression of fly Notch with an *O*-fucosylation site mutation at EGF12 was able to respond to Dl during embryonic neurogenesis and rescued the neurogenic phenotype of a *Notch* null allele (Lei et al., 2003), suggesting that the glycan decorating this site is dispensable for Dl-mediated Notch signaling. However, we find that when *N[12A]* is expressed at near-endogenous levels by *N[gt-12A]*, it is not able to rescue the neurogenic

phenotype in *Notch* null embryos (Figure 3). Since Fng does not play a role in embryonic neurogenesis (Haines and Irvine, 2003), this effect is likely to be due to the absence of fuc from EGF12. *N[gt-12T]*, which changes the amino acid but still allows *O*-fucosylation at EGF12, completely rescues this phenotype (Figures S4D–S4F'). We conclude that a single, unmodified fuc monosaccharide on EGF12 of Notch is essential for embryonic neurogenesis in *Drosophila* at endogenous levels of Notch. Notably, mice homozygous for *Notch1[12f]*, which are equivalent to *N[−]/Y*; *N[gt-12A]/+* flies in our studies, exhibit impaired T cell development but do not show any abnormalities during embryonic development (Ge and Stanley, 2008). This suggests that the contribution of *O*-fuc glycans on individual Notch EGF repeats in each *in vivo* context depends not only on the specific site but also on other factors, including the levels of the Notch receptor and the presence or absence of Fng proteins.

N[gt-12A] showed a significant rescue of wing vein thickening in *N[+/−]* flies (full rescue in 57% of the wings, partial rescue in the remaining 43%; Figure 4). This is in contrast to the embryonic neurogenesis in *N[−]/Y* males, in which this mutation showed no rescue of the neurogenic phenotype. Multiple lines of evidence suggest that this difference is due to the Fng modification of EGF8 and also EGF9 to a lesser degree. First, unlike embryonic neurogenesis, Fng is involved in wing vein development (Correia et al., 2003; Ishio et al., 2015). Second, despite the significant decrease in Dl binding of N-12A, our aggregation and *in vitro* assays indicate that Fng is able to robustly increase the binding of N-12A with Dl (Figures 2 and 5), in agreement with previous *in vitro* binding assays (Lei et al., 2003). Third, the simultaneous loss of the *O*-fucosylation site in EGF8 and to some extent EGF9 decreases the ability of N-12A to rescue the wing vein phenotype of *N[+/−]* females (Figure 4). Fourth, the the ability of N-8V12A to mediate the aggregation of S2 cells with S2-Dl cells cannot be enhanced by Fng any longer (Figure 5). Fifth, the wing vein-thickening phenotype of *N[+/−]*; *N[gt-12A]*, *N [+/−]; N[gt-8V12A]*, and *N[+/−]*; *N[gt-9V12A]* animals can be modified by altering the *fng* gene dosage (Figure 4). These data suggest that (1) in the absence of Fng, *O*-fuc on EGF12 is essential for Dl-Notch signaling required for embryonic neurogenesis and cannot be compensated for by *O*-fuc on other EGF repeats, and (2) in the presence of Fng, GlcNAc on *O*-fucosylated EGF12 contributes to Dl-Notch signaling, but is largely redundant with GlcNAc-fuc-*O* on EGF8 and partially redundant with that on EGF9. These data are in agreement with the previous observation that the *O*-fuc modification and GlcNAc elongation of EGF12 and EGF8 together facilitate Fng-mediated increase in DLL1-NOTCH1 signaling in mammalian cell-based assays (Kakuda and Haltiwanger, 2017).

Quantitative assays in mammalian cells and genetic interaction studies in flies indicate that Fng proteins can affect the *cis*-interactions between Notch and ligands similar to their effect on Notch-ligand *trans*-interactions (promote Notch-Dl/DLL1 *cis*-interactions, inhibit Notch-Ser/JAG *cis*-interactions) (LeBon et al., 2014). Moreover, it has been reported that in the fly wing imaginal discs, Notch *cis*-inhibits Ser and decreases its ability to activate signaling in neighboring cells (Becam et al., 2010). However, it was not known how Fng regulates this process. Our data indicate that upon mutating the *O*-fuc sites on both EGF8 and EGF12 (but not individually), Notch *cis*-inhibits Ser and impairs normal wing margin formation. Moreover, cell aggregation assays suggest that mutating these two sites impairs the ability of Fng to block the *cis*-interaction between Notch and Ser. Based on these data, we propose

that during *Drosophila* wing margin formation, a key role of Fng is to reduce the Notch-mediated *cis*-inhibition of Ser by adding GlcNAc to *O*-fucosylated EGF8 and EGF12. It has recently been hypothesized that during inner ear hair cell development, LFNG and MFNG block the *cis*-inhibition of JAG1 and JAG2 by NOTCH1, thereby allowing these ligands to induce Notch signaling in neighboring cells (Basch et al., 2016). We suggest that a non-cell-autonomous loss of Notch signaling due to impaired ligand *cis*-inhibition by Notch should be considered as a possibility when interpreting *Fringe* loss-of-function phenotypes *in vivo*.

STAR★METHODS

LEAD CONTACT AND MATERIALS AVAILABILITY

Further information and requests for resources and reagents should be directed to and will be fulfilled by the Lead Contact, Hamed Jafar-Nejad (hamedjn@bcm.edu). Constructs and fly lines generated in this study will be shared upon request.

EXPERIEMENTAL MODEL AND SUBJECT DETAILS

Following *Drosophila* strains were used in the study: (1) y w (Bloomington *Drosophila* Stock Center); (2) w; noc^{Sco}/CyO; TM3, Sb^1/TM6, Tb^1 (Lee et al., 2013); (3) y w, N^{55e11}/FM7c, B^1, (4) y w N^{54l9} FRT19A/FM7c, B^1, (5) y w Ubx-FLP Tub-GAL80 FRT19A; Act-GAL4 UAS-GFP^{nls}/CyO, y^+ and (6) PBac{$N^{gt\text{-}wt}$}VK22 (Leonardi et al., 2011); (7) PBac{N^{gt-5V}}VK22, (8) PBac{N^{gt-8V}}VK22, (9) PBac{N^{gt-9V}}VK22, (10) PBac{N^{gt-12A}}VK22, (11) PBac{$N^{gt-8V9V}$}VK22, (12) PBac{$N^{gt-8V12A}$}VK22, (13) PBac{$N^{gt-9V12A}$}VK22, (14) PBac{N^{gt-9S}}VK22, (15) PBac{N^{gt-12T}}VK22 and (16) PBac{$Ser^{gt\text{-}wt}$}VK31 (this study), (15) P{$Dl^{gt\text{-}wt}$}attP2 (LeBon et al., 2014), (16) PBac{CH321–87O20}VK37 (fng duplication strain, GenetiVision), (17) fng^{L73}/TM3, Sb^1 (BDSC#9416; (Correia et al., 2003)). All crosses in the study were performed on standard media.

METHOD DETAILS

Expression Plasmids Used for Cell-Based Binding Assays—The plasmid expressing EGF repeats 1–36 from *Drosophila* Notch fused to a C-terminal CD2 domain (N-CD2) was provided by Dr. Shinya Yamamoto (Baylor College of Medicine) and has been previously described (Brückner et al., 2000; Yamamoto et al., 2012). The plasmid expressing *Drosophila* Fng was generated by cloning Fng from a plasmid provided by Dr. Ken Irvine (Rutgers University; (Okajima et al., 2003)) into the pMT-V5His plasmid (Thermo Fisher) using primers (forward) GGAATTCGATGATGAGCCT GACTGTGCTCTCGC and (reverse) GCTCTAGATTTCTGGGCGGGCAGAAGCT. Plasmids encoding the extracellular domains (amino acids 1–592 from Dl and amino acids 1–1213 from Ser) of the ligands with C-terminal Myc-6xHis tags were generated by inserting sequences encoding the Myc-6xHis tag with a stop codon immediately after the respective extracellular domains in pMT-Dl-AP and pMT-Ser-AP plasmids, also gifts from Dr. Ken Irvine (Rutgers University). To generate the plasmid expressing GFP used in the cell-based binding assays, EGFP was cloned from the EGFP-N1 plasmid (Clontech) and inserted into pMT-V5His empty vector using primers (forward) GGAATTCGATGGTGAGCAAGGGCGA and (reverse) GCTCTAGACGCTTGTACAGCTCGTCCATGC.

Production and Purification Of Dl and Ser Protein for Binding Assays—Stable S2 cell lines expressing Dl or Ser ligands with C-terminal Myc-6xHis tags were generated by transfecting 20 μg of plasmid using the calcium phosphate transfection method as described in the Calcium Phosphate Transfection Kit (Invitrogen), although the buffers used were made in-lab. Stable cell lines expressing ligands were maintained with 50 μg/ml Blasticidin (Invitrogen) selection. To generate protein used in binding assays, cells were induced with 0.7 mM $CuSO_4$ in complete medium for three days. Batches of ligand protein were purified from about 100 mL of clarified medium with 1 mL packed Ni-NTA resin (QIAGEN). Resin was washed with 10 mM imidazole, 0.5M NaCl in PBS and proteins were eluted with 250 mM imidazole in PBS. Elutions were concentrated and imidazole was diluted with PBS using Amicon centrifugal filters (Millipore). Protein was aliquoted and stored at −80°C.

Site-Directed Mutagenesis of N-CD2 and Fng for Binding Assays—N-CD2 with mutant *O*-fucosylation sites in the EGF repeats of and the catalytically inactive Fringe-DEE mutant were generated using QuikChange II XL Site-Directed Mutagenesis Kit (Agilent Technologies) according to the manufacture's protocol. *O*-fuc site mutations were designed to change the modified threonine (T) or Serine (S) within the *O*-fucosylation consensus sequence (C^2xxxx(S/T)C^3 (Harvey et al., 2016; Rana and Haltiwanger, 2011)) to Valine (V) or Alanine (A), respectively. Mutations were confirmed by DNA sequencing. Primers used for mutagenesis are listed in Table S1.

Cell-Based Ligand Binding Assays and Flow Cytometry—S2 cells were transfected with plasmids encoding N-CD2 or *O*-fuc site N-CD2 mutants for cell-based binding assays using Effectene Reagent (QIAGEN) following the manufacturer's instructions. Briefly, 1 μg of Notch-CD2 or empty vector control was transfected with 0.2 μg of pMT-GFP plasmid in order to monitor transfection efficiency and allow us to gate out untransfected cells from analysis. Varying amounts of Fng plasmid or control empty vector were also transfected when we tested the effects of Fng. DNA was diluted in 150 μL of Effectene Buffer. Enhancer reagent was mixed in a 1:7 DNA to reagent ratio for 5 minutes, then Effectene was added in a ratio of 1:9 for 10 minutes. The DNA Effectene solutions were mixed with 1ml of complete medium then directly mixed with 1×10^6 suspended cells in 1ml medium and plated in 35 mm dishes. Cells were induced with 0.7mM $CuSO_4$ for 4 hours following the transfection and cultured for 3 days.

N-CD2 expressing S2 cells were collected and washed in cold binding buffer (HBSS, 1mM CaCl2, 1% BSA, 0.05% sodium azide). For detecting cell surface expression of N-CD2 or *O*-fuc site mutants, cells were labeled with anti-CD2 antibody, which recognizes the extracellular portion of the CD2 protein, (1:100) in 50 μL binding buffer for 1 hour at 4°C. Cells were washed with 1 mL of binding buffer, then labeled with PE-conjugated goat anti-mouse antibody (1:100) in 100 μL binding buffer for 1 hour at 4°C. Cells were washed twice with 1 mL binding buffer, then analyzed with flow cytometry.

For ligand binding assays, ligand protein was clustered with PE-conjugated mouse anti-myc (1:20) in 50 μL binding buffer for 1 hour at 4°C (clustering of ligand enhances avidity, mimicking binding to cell-surface ligand). Clustered ligand solutions were then mixed with

the N-CD2 expressing cells for 1 hour at 4°C. After binding with PE-clustered ligands, cells were washed twice with 1 mL binding buffer, then analyzed with flow cytometry.

For flow cytometric analyses, cells were then resuspended in about 300–400 μL binding buffer and filtered into flow cytometry tubes with cell strainer caps (Falcon). Cellular debris were excluded by gating. GFP-positive cells were gated before analyzing cell surface expression or ligand binding. Data were acquired and analyzed using a BD FACSCalibur flow cytometer (BD Biosciences) with BD CellQuestPro (BD Biosciences) and FlowJo (Tree Star) software. S2 cells transfected with control empty vector were generated for each experiment, and the mean fluorescence intensities of labeling from these control cells were subtracted from each data point.

Antibodies for Flow Cytometric Analyses and Western Blotting—Antibodies used for western blotting or labeling for flow cytometric analyses include: mouse anti-CD2 (OX-34 clone, Bio-Rad); mouse anti-Notch (F461.3B, DSHB); rabbit anti-V5 (Sigma); HRP-conjugated goat anti-mouse (Jackson ImmunoResearch); Alexa Fluor680 rabbit anti-mouse (Invitrogen); IRDye700 goat anti-rabbit (Rockland Immunochemicals); PE-conjugated goat anti-mouse (Life Technologies); PE-conjugated mouse anti-myc (9E10 clone, R&D systems). Western blots using fluorescent probes were visualized using the Odyssey system (LI-COR), while western blots with peroxidase conjugated probes were detected by enhanced chemiluminescence blotting substrate (Thermo Scientific) and film development.

Site-Directed Mutagenesis of PMT-NOTCH for Cell Aggregation Assays—The pMT expression plasmid encoding *Drosophila* Notch (pMT-Notch; *Drosophila* Genome Research Center stock number 1022, https://dgrc.bio.indiana.edu/product/View?product=1022) was used as template for making mutants eliminating the O-fucosylation site in EGF repeats 8 and 12.

For the mutant EGF8 TV, the corresponding two nucleotide mutations (underlined in primers) were introduced by PCR-based site-directed mutagenesis with this plasmid and the following primers: 5′-CGGAGCCGTCTGTACAAACACTCACGGATCG-3′ and 5′-TGTACAGACGGCTCCGTTCTGGCACACCGG-3′.

For the mutant EGF12 SA, the corresponding nucleotide mutation (underlined in primers) was introduced by PCR-based site-directed mutagenesis with this plasmid and the following primers: 5′-CGAGGGAGCTTGCCTGGATGATCCGG-3′ and 5′-CAGG CAAGCTCCCTCGTTCTGGCATGG-3′.

Double mutants were generated by iteration of the above. Successful incorporation of the mutation was confirmed by direct DNA sequencing.

Generation of Genomic Transgenes—To generate the *O*-fucosylation site mutant *Notch* transgenes, we used the gap-repair mutagenesis strategy, as described previously (Leonardi et al., 2011; Leonardi and Jafar-Nejad, 2014). To generate the *Notch*-5V transgene, we used the $N^{4,5}$*/CS-attB-P[acman]-*Ap^{R} construct, in which a 213 bp region in

the *Notch* genomic locus encoding EGF4 and EGF5 is replaced by the CAT/SacB (chloramphenicol acetyl transferase/sucrose sensitivity; CS) selection cassette (Leonardi et al., 2011; Leonardi and Jafar-Nejad, 2014). The following primers were used to introduce a TV mutation in the *O*-fucosylation site of EGF5 in the *LA-EGF4,5-RA-pCR-Blunt II-TOPO* targeting vector (LA and RA are left and right homology arms, respectively):

EGF5-TV-for: GCAAATACGGCGGCGTATGTGTCAACACCC

EGF5-TV-rev: GGGTGTTGACACATACGCCGCCGTATTTGC

Recombineering was then used to replace the CAT/SacB cassette in the $N^{4,5}$/*CS-attB-P[acman]-Ap*^{R} construct with the 213 bp insert from the *pCR-Blunt II-TOPO-EGF4,5V* targeting vector resulting from the above-mentioned mutagenesis. The final construct (*N[gt-5V]-attB-P[acman]-Ap*^{R} was verified by EcoRI fingerprinting and sequencing of all exons and exon-intron junctions.

For EGF9 and EGF12 single mutants (EGF9V, EGF9S, EGF12A and EGF12T), a similar strategy was used, with N^{10-35}/*CS-attB-P [acman]-Ap*^{R} as the template construct (Leonardi et al., 2011; Leonardi and Jafar-Nejad, 2014). The coding sequence for EGF8 and EGF9 are located in the left homology arm of this construct and can be targeted. The following primers were used to introduce the intended mutations in the *LA-EGF10_35-RA-pCR-Blunt II-TOPO* targeting vector:

EGF9-TV-for: GTTTCTACGGAGCCGTGTGCATCGATGGCG

EGF9-TV-rev: CGCCATCGATGCACACGGCTCCGTAGAAAC

EGF9-TS-for: GTTTCTACGGAGCCTCGTGCATCGATGGCG

EGF9-TS-rev: CGCCATCGATGCACGAGGCTCCGTAGAAAC

EGF12-SA-for: TGCCAGAACGAGGGAGCTTGCCTGGATGATC

EGF12-SA-rev: GATCATCCAGGCAAGCTCCCTCGTTCTGGCA

EGF12-ST-for: TGCCAGAACGAGGGAACTTGCCTGGATGATC

EGF12-ST-rev: GATCATCCAGGCAAGTTCCCTCGTTCTGGCA

A 13-bp sequence immediately 3′ to the coding sequence for EGF8 *O*-fucosylation site is identical to another 13-bp sequence in the coding sequence for EGF7. This duplicated sequence prevented us from performing a conventional site-directed mutagenesis on the *O*-fucosylation site in EGF8 in the *LA-EGF10_35-RA-pCR-Blunt II-TOPO* targeting vector. We therefore used PCR to generate two fragments of the insert in the above-mentioned vector, each containing one of the two copies of the 13-bp region. We then used site-directed mutagenesis to introduce a TV mutation in EGF8 and performed a triple-ligation to assemble the two fragments and the vector backbone into the *LA-EGF10_35-EGF8V-RA-pCR-Blunt II-TOPO* targeting vector. The following primers were used:

3′−16EGF-XbaI: CCCTCTAGAGCAGTAGGCATCGAAAAGGCTATC

5′−16EGF-KpnI: CCGGTACCTTAGTCAGCGAGGGGAGTGGG

16EGF-BsaI-for: ACAGGTCTCCACCTGCCGCTGTCCACCG

16EGF-BsaI-rev: ACAGGTCTCCAGGTGTAGTCCGAGATGCCATC

EGF8-TV-for: TGCCAGAACGGAGCCGTCTGTACAAACACTCAC

EGF8-TV-rev: GTGAGTGTTTGTACAGACGGCTCCGTTCTGGCA

Similar strategies were used to generate double mutant versions of the *LA-EGF10_35-RA-pCR-Blunt II-TOPO* targeting vector. Recombineering was then used to exchange the CAT/SacB cassette in the N^{10-35}*/CS-attB-P[acman]-Ap*^{R} construct with EGF10_35 fragments containing individual or double-EGF repeat mutations, as described above. After EcoRI fingerprinting and sequencing to verity the presence of the mutations and the integrity of all *Notch* exons and exon-intron boundaries, φC31-mediated transgenesis was used to integrate all transgenes into the *VK22* docking site on the second chromosome (Venken et al., 2006). To generate a *Ser* genomic transgene on the third chromosome, the BAC clone *attB-P[acman]-CmR-CH321–69C08* (Venken et al., 2009) was inserted into the *VK31* docking site by φC31-mediated transgenesis. This BAC contains the regulatory elements required for *Ser* expression, based on our previous work in which we used a second chromosome insertion of this BAC in genetic interaction studies (LeBon et al., 2014). All embryo injections were performed by GenetiVision (Houston, TX).

Genetic Rescue and Gene Doasge Experiements—For the rescue and gene dosage experiments, N^{55e11}*/FM7c* females were crossed with *y w/Y;* N^{gt}*/CyO* males and raised at room temperature to obtain N^{55e11}/+, N^{55e11}/+; N^{gt}/+ females and N^{55e11}*/Y;* N^{gt}/+ males based on the absence of Bar eye and curly wing phenotypes. N^{55e11}*/FM7;* N^{gt}*/CyO* females were crossed with $Ser^{gt\text{-}wt}$*/TM3,* Sb^{1} and $Dl^{gt\text{-}wt}$*/TM6,*Tb^{1} males and raised at room temperature to obtain N^{55e11}/+*;* N^{gt}/+*;* $Ser^{gt\text{-}wt}$/+ and N^{55e11}/+*;* N^{gt}/+*;* $Dl^{gt\text{-}wt}$/+ females, respectively, based on the absence of Bar eye and curly wing or Tubby phenotypes.

***In Vivo* Clonal Analysis for Cell Surface Expression Level of Notch—**To examine the effects of *O*-fuc mutations on the surface expression of Notch *in vivo*, we used the MARCM system (Lee and Luo, 2001) to generate animals with clones of the *Notch* null allele *N[54I9]*, with or without a copy of wild-type or mutant *N[gt]*. To generate *Notch* null MARCM clones, *y w Ubx-FLP Tub-GAL80 FRT19A; Act-GAL4 UAS-GFP*^{nls}*/CyO,* y^{+} males were crossed to *y w* N^{54l9} *FRT19A/FM7c* or N^{54l9} *FRT19A/FM7c;* N^{gt}/+ females. Animals were raised at room temperature until the second instar larval period and were then transferred to 30°C. Then after, detergent-free immunostainings was performed to examine the cell surface level of Notch protein, as reported previously (Leonardi et al., 2011). Since *N[54I9]* is a protein null allele (Figures S3A–S3A”), the only source of surface Notch in *N[54I9]* clones will be that expressed from wild-type or mutant *Notch* transgenes. Considering the potential batch-to-batch variations in staining intensity, for each sample we generated the plot profiles of the signal intensity for a box covering both clonal area and the

neighboring control area equally and calculated the relative signal intensity of the clone to control area in each sample as a measure of the cell surface level of Notch (Figures S3B–S3I"). Plot profile intensity was measured using ImageJ 1.47. Confocal images were scanned using a Leica TCS-SP5 microscope and processed with Amira5.2.2. Images were processed with Adobe Photoshop CS5; Figures were assembled in Adobe Illustrator CS5.

Dissections, Staining, Image Acquisition and Processing—Dissection and staining were performed using standard protocols. Embryos were collected at stage 12–14 (10–13 hours). Wing imaginal discs were dissected from late third instar larvae. Notch surface staining was performed without using detergent. Antibodies were mouse anti-NECD 1:100 and rat anti-Elav 1:200 (Developmental Studies Hybridoma Bank), goat anti-mouse Alexa Fluor-488 and goat anti-rat Cy3-conjugated 1:500 (Jackson ImmunoResearch Laboratories). Confocal images were scanned using a Leica TCS-SP5 microscope and processed with Amira5.2.2. Images were processed with Adobe Photoshop CS5; Figures were assembled in Adobe Illustrator CS5.

S2 Cell Culture and Cell Aggregation Assays—S2 cells (Invitrogen) were cultured in Schneider's *Drosophila* Medium (Lonza) supplemented with 10% fetal bovine serum and penicillin-streptomycin (100 U/mL). For S2-N and S2-Dl stable cell lines (DGRC, Bloomington, USA), 200 nM methotrexate (Sigma-Aldrich) was added. For S2-Ser^{Tom} stable cell line, 100 μg/mL hygromycin B was used. Cells were cultured for 24 hours at 24 ± 1°C prior to induction with CuS04 (0.7 mM). Cells were incubated with CuSO4 for 1–2 days and then used in aggregation assays. For each aggregation assay, 2.5×10^5 of the stable S2-Dl or S2-N cells were mixed with 5×10^5 of S2 cells transiently transfected with 2 μg total of either *pBluescript* (control) or *pBluescript* and *pMT-Notch* (S2-N) and *pBluescript* and *pMT-Ser* (S2-Ser) or *pBluescript, pMT-Ser* and *pMT-Notch* (S2-Ser-N) and *pMT-Ser, pMT-Notch* and *pMT-fng* (S2-Ser-N-Fng) using 3 μL of FuGENE HD (Promega). For all transiently transfected S2 cells expressing *trans*-Notch, one μg of *pMT-Notch* was used. For the S2 cell expressing Ser and *cis*-Notch, 1.2 μg of *pMT-Ser* and 0.6 μg of *pMT-Notch* were used. A ratio of 1:2 was used for Fng and Notch co-expression all aggregation assays. After mixing, cells were gently shaken at 150 rpm to allow aggregation. Images of aggregate formation were taken after 5 minutes. The number of cell aggregates was quantified using a hemocytometer after 5 minutes of aggregation. Each assay was repeated at least three times. *P*-values were determined either by Student's t test or by One-Way ANOVA followed by Dunnett's post hoc test.

QUANTIFICATION AND STATISTICAL ANALYSIS

Statistical parameters including the sample sizes and replicates, data plotted (mean ± SD), *P* values, and statistical tests used are mentioned in Figure Legends. Statistical analyses were performed using Graphpad Prism 6. Data were analyzed by Student's t test or by one-way ANOVA with the Dunett' Post hoc multiple comparisons test.

DATA AND CODE AVAILABILITY

This study did not generate/analyze any datasets/code.

Supplementary Material

Refer to Web version on PubMed Central for supplementary material.

ACKNOWLEDGMENTS

We acknowledge support from the NIH (R01GM084135 and R35GM130317 to H.J.-N., R01GM061126 to R.S.H.) and the Mizutani Foundation for Glycoscience (grant #110071 to H.J.-N.). We thank the Bloomington *Drosophila* Stock Center (NIH P40OD018537) and the Developmental Studies Hybridoma Bank for the reagents; the Microscopy Core of the Baylor College of Medicine (BCM) Intellectual and Developmental Disabilities Research Center (IDDRC) (supported by 1U54HD083092 from the Eunice Kennedy Shriver National Institute of Child Health and Human Development [NICHD/NIH]), the BCM Integrated Microscopy Core (supported by NCI-CA125123, NIDDK-56338–13/15, and CPRIT-RP150578 and the John S. Dunn Gulf Coast Consortium for Chemical Genomics), and Drs. Shinya Yamamoto and Ken Irvine for the plasmids. We also want to thank members of the Haltiwanger and Jafar-Nejad labs for discussion and comments.

REFERENCES

Andrawes MB, Xu X, Liu H, Ficarro SB, Marto JA, Aster JC, and Blacklow SC (2013). Intrinsic selectivity of Notch 1 for Delta-like 4 over Delta-like 1. J. Biol. Chem 288, 25477–25489. [PubMed: 23839946]

Artavanis-Tsakonas S, and Muskavitch MA (2010). Notch: the past, the present, and the future. Curr. Top. Dev. Biol 92, 1–29. [PubMed: 20816391]

Artavanis-Tsakonas S, Muskavitch MA, and Yedvobnick B (1983). Molecular cloning of Notch, a locus affecting neurogenesis in *Drosophila* melanogaster. Proc. Natl. Acad. Sci. USA 80, 1977–1981. [PubMed: 6403942]

Baek C, Freem L, Goïame R, Sang H, Morin X, and Tozer S (2018). Mib1 prevents Notch Cis-inhibition to defer differentiation and preserve neuroepithelial integrity during neural delamination. PLoS Biol. 16, e2004162. [PubMed: 29708962]

Basch ML, Brown RM 2nd, Jen HI, Semerci F, Depreux F, Edlund RK, Zhang H, Norton CR, Gridley T, Cole SE, et al. (2016). Fine-tuning of Notch signaling sets the boundary of the organ of Corti and establishes sensory cell fates. eLife 5, e19921. [PubMed: 27966429]

Becam I, Fiuza UM, Arias AM, and Milán M (2010). A role of receptor Notch in ligand cis-inhibition in *Drosophila*. Curr. Biol 20, 554–560. [PubMed: 20226663]

Bray SJ (2006). Notch signalling: a simple pathway becomes complex. Nat. Rev. Mol. Cell Biol 7, 678–689. [PubMed: 16921404]

Brückner K, Perez L, Clausen H, and Cohen S (2000). Glycosyltransferase activity of Fringe modulates Notch-Delta interactions. Nature 406, 411–415. [PubMed: 10935637]

Cohen B, Bashirullah A, Dagnino L, Campbell C, Fisher WW, Leow CC, Whiting E, Ryan D, Zinyk D, Boulianne G, et al. (1997). Fringe boundaries coincide with Notch-dependent patterning centres in mammals and alter Notch-dependent development in *Drosophila*. Nat. Genet 16, 283–288. [PubMed: 9207795]

Cordes R, Schuster-Gossler K, Serth K, and Gossler A (2004). Specification of vertebral identity is coupled to Notch signalling and the segmentation clock. Development 131, 1221–1233. [PubMed: 14960495]

Correia T, Papayannopoulos V, Panin V, Woronoff P, Jiang J, Vogt TF, and Irvine KD (2003). Molecular genetic analysis of the glycosyltransferase Fringe in *Drosophila*. Proc. Natl. Acad. Sci. USA 100, 6404–6409. [PubMed: 12743367]

de Celis JF, and Bray S (1997). Feed-back mechanisms affecting Notch activation at the dorsoventral boundary in the *Drosophila* wing. Development 124, 3241–3251. [PubMed: 9310319]

de Celis JF, and Bray SJ (2000). The Abruptex domain of Notch regulates negative interactions between Notch, its ligands and Fringe. Development 127, 1291–1302. [PubMed: 10683181]

de Celis JF, Barrio R, del Arco A, and García-Bellido A (1993). Genetic and molecular characterization of a Notch mutation in its Delta- and Serrate-binding domain in *Drosophila*. Proc. Natl. Acad. Sci. USA 90, 4037–4041. [PubMed: 8483919]

de Celis JF, Bray S, and Garcia-Bellido A (1997). Notch signalling regulates veinlet expression and establishes boundaries between veins and interveins in the *Drosophila* wing. Development 124, 1919–1928. [PubMed: 9169839]

Doherty D, Feger G, Younger-Shepherd S, Jan LY, and Jan YN (1996). Delta is a ventral to dorsal signal complementary to Serrate, another Notch ligand, in *Drosophila* wing formation. Genes Dev. 10, 421–434. [PubMed: 8600026]

Evrard YA, Lun Y, Aulehla A, Gan L, and Johnson RL (1998). lunatic fringe is an essential mediator of somite segmentation and patterning. Nature 394, 377–381. [PubMed: 9690473]

Fehon RG, Kooh PJ, Rebay I, Regan CL, Xu T, Muskavitch MA, and Artavanis-Tsakonas S (1990). Molecular interactions between the protein products of the neurogenic loci Notch and Delta, two EGF-homologous genes in *Drosophila*. Cell 61, 523–534. [PubMed: 2185893]

Fleming RJ, Hori K, Sen A, Filloramo GV, Langer JM, Obar RA, Artavanis-Tsakonas S, and Maharaj-Best AC (2013). An extracellular region of Serrate is essential for ligand-induced cis-inhibition of Notch signaling. Development 140, 2039–2049. [PubMed: 23571220]

Ge C, and Stanley P (2008). The O-fucose glycan in the ligand-binding domain of Notch1 regulates embryogenesis and T cell development. Proc. Natl. Acad. Sci. USA 105, 1539–1544. [PubMed: 18227520]

Geffers I, Serth K, Chapman G, Jaekel R, Schuster-Gossler K, Cordes R, Sparrow DB, Kremmer E, Dunwoodie SL, Klein T, and Gossler A (2007). Divergent functions and distinct localization of the Notch ligands DLL1 and DLL3 in vivo. J. Cell Biol 178, 465–476. [PubMed: 17664336]

Haines N, and Irvine KD (2003). Glycosylation regulates Notch signalling. Nat. Rev. Mol. Cell Biol 4, 786–797. [PubMed: 14570055]

Haltom AR, and Jafar-Nejad H (2015). The multiple roles of epidermal growth factor repeat O-glycans in animal development. Glycobiology 25, 1027–1042. [PubMed: 26175457]

Harvey BM, and Haltiwanger RS (2018). Regulation of Notch Function by O-Glycosylation. Adv. Exp. Med. Biol 1066, 59–78. [PubMed: 30030822]

Harvey BM, Rana NA, Moss H, Leonardi J, Jafar-Nejad H, and Haltiwanger RS (2016). Mapping Sites of O-Glycosylation and Fringe Elongation on *Drosophila* Notch. J. Biol. Chem 291, 16348–16360. [PubMed: 27268051]

Heitzler P, and Simpson P (1991). The choice of cell fate in the epidermis of *Drosophila*. Cell 64, 1083–1092. [PubMed: 2004417]

Henrique D, Hirsinger E, Adam J, Le Roux I, Pourquié O, Ish-Horowicz D, and Lewis J (1997). Maintenance of neuroepithelial progenitor cells by Delta-Notch signalling in the embryonic chick retina. Curr. Biol 7, 661–670. [PubMed: 9285721]

Hicks C, Johnston SH, diSibio G, Collazo A, Vogt TF, and Weinmaster G (2000). Fringe differentially modulates Jagged1 and Delta1 signalling through Notch1 and Notch2. Nat. Cell Biol 2, 515–520. [PubMed: 10934472]

Huppert SS, Jacobsen TL, and Muskavitch MA (1997). Feedback regulation is central to Delta-Notch signalling required for *Drosophila* wing vein morphogenesis. Development 124, 3283–3291. [PubMed: 9310323]

Irvine KD, and Wieschaus E (1994). fringe, a Boundary-specific signaling molecule, mediates interactions between dorsal and ventral cells during *Drosophila* wing development. Cell 79, 595–606. [PubMed: 7954826]

Ishio A, Sasamura T, Ayukawa T, Kuroda J, Ishikawa HO, Aoyama N, Matsumoto K, Gushiken T, Okajima T, Yamakawa T, and Matsuno K (2015). O-fucose monosaccharide of *Drosophila* Notch has a temperature-sensitive function and cooperates with O-glucose glycan in Notch transport and Notch signaling activation. J. Biol. Chem 290, 505–519. [PubMed: 25378397]

Jacobsen TL, Brennan K, Arias AM, and Muskavitch MA (1998). Cis-interactions between Delta and Notch modulate neurogenic signalling in *Drosophila*. Development 125, 4531–4540. [PubMed: 9778511]

Johnston SH, Rauskolb C, Wilson R, Prabhakaran B, Irvine KD, and Vogt TF (1997). A family of mammalian Fringe genes implicated in boundary determination and the Notch pathway. Development 124, 2245–2254. [PubMed: 9187150]

Kakuda S, and Haltiwanger RS (2017). Deciphering the Fringe-Mediated Notch Code: Identification of Activating and Inhibiting Sites Allowing Discrimination between Ligands. Dev. Cell 40, 193–201. [PubMed: 28089369]

Kelley MR, Kidd S, Deutsch WA, and Young MW (1987). Mutations altering the structure of epidermal growth factor-like coding sequences at the *Drosophila* Notch locus. Cell 51, 539–548. [PubMed: 3119223]

Klein T, Brennan K, and Arias AM (1997). An intrinsic dominant negative activity of serrate that is modulated during wing development in *Drosophila*. Dev. Biol 189, 123–134. [PubMed: 9281342]

Lawrence N, Klein T, Brennan K, and Martinez Arias A (2000). Structural requirements for notch signalling with delta and serrate during the development and patterning of the wing disc of *Drosophila*. Development 127, 3185–3195. [PubMed: 10862754]

LeBon L, Lee TV, Sprinzak D, Jafar-Nejad H, and Elowitz MB (2014). Fringe proteins modulate Notch-ligand cis and trans interactions to specify signaling states. eLife 3, e02950. [PubMed: 25255098]

Lee T, and Luo L (2001). Mosaic analysis with a repressible cell marker (MARCM) for Drosophila neural development. Trends Neurosci. 24, 251–254. [PubMed: 11311363]

Lee TV, Sethi MK, Leonardi J, Rana NA, Buettner FF, Haltiwanger RS, Bakker H, and Jafar-Nejad H (2013). Negative regulation of notch signaling by xylose. PLoS Genet. 9, e1003547. [PubMed: 23754965]

Lee TV, Pandey A, and Jafar-Nejad H (2017). Xylosylation of the Notch receptor preserves the balance between its activation by trans-Delta and inhibition by cis-ligands in Drosophila. PLoS Genet. 13, e1006723. [PubMed: 28394891]

Lei L, Xu A, Panin VM, and Irvine KD (2003). An O-fucose site in the ligand binding domain inhibits Notch activation. Development 130, 6411–6421. [PubMed: 14627724]

Leonardi J, and Jafar-Nejad H (2014). Structure-function analysis of *Drosophila* Notch using genomic rescue transgenes. Methods Mol. Biol 1187, 29–46. [PubMed: 25053479]

Leonardi J, Fernandez-Valdivia R, Li YD, Simcox AA, and Jafar-Nejad H (2011). Multiple O-glucosylation sites on Notch function as a buffer against temperature-dependent loss of signaling. Development 138, 3569–3578. [PubMed: 21771811]

Luca VC, Kim BC, Ge C, Kakuda S, Wu D, Roein-Peikar M, Haltiwanger RS, Zhu C, Ha T, and Garcia KC (2017). Notch-Jagged complex structure implicates a catch bond in tuning ligand sensitivity. Science 355, 1320–1324. [PubMed: 28254785]

Mašek J, and Andersson ER (2017). The developmental biology of genetic Notch disorders. Development 144, 1743–1763. [PubMed: 28512196]

Micchelli CA, Rulifson EJ, and Blair SS (1997). The function and regulation of cut expression on the wing margin of *Drosophila*: Notch, Wingless and a dominant negative role for Delta and Serrate. Development 124, 1485–1495. [PubMed: 9108365]

Moloney DJ, Panin VM, Johnston SH, Chen J, Shao L, Wilson R, Wang Y, Stanley P, Irvine KD, Haltiwanger RS, and Vogt TF (2000a). Fringe is a glycosyltransferase that modifies Notch. Nature 406, 369–375. [PubMed: 10935626]

Moloney DJ, Shair LH, Lu FM, Xia J, Locke R, Matta KL, and Haltiwanger RS (2000b). Mammalian Notch1 is modified with two unusual forms of O-linked glycosylation found on epidermal growth factor-like modules. J. Biol. Chem 275, 9604–9611. [PubMed: 10734111]

Nandagopal N, Santat LA, and Elowitz MB (2019). Cis-activation in the Notch signaling pathway. eLife 8, e37880. [PubMed: 30628888]

Okajima T, and Irvine KD (2002). Regulation of notch signaling by o-linked fucose. Cell 111, 893–904. [PubMed: 12526814]

Okajima T, Xu A, and Irvine KD (2003). Modulation of notch-ligand binding by protein O-fucosyltransferase 1 and fringe. J. Biol. Chem 278, 42340–42345. [PubMed: 12909620]

Pandey A, and Jafar-Nejad H (2018). Cell Aggregation Assays to Evaluate the Binding of the Drosophila Notch with Trans-Ligands and its Inhibition by Cis-Ligands. J. Vis. Exp (131) 10.3791/56919.

Panin VM, Papayannopoulos V, Wilson R, and Irvine KD (1997). Fringe modulates Notch-ligand interactions. Nature 387, 908–912. [PubMed: 9202123]

Rana NA, and Haltiwanger RS (2011). Fringe benefits: functional and structural impacts of O-glycosylation on the extracellular domain of Notch receptors. Curr. Opin. Struct. Biol 21, 583–589. [PubMed: 21924891]

Rebay I, Fleming RJ, Fehon RG, Cherbas L, Cherbas P, and Artavanis-Tsakonas S (1991). Specific EGF repeats of Notch mediate interactions with Delta and Serrate: implications for Notch as a multifunctional receptor. Cell 67, 687–699. [PubMed: 1657403]

Robinow S, and White K (1991). Characterization and spatial distribution of the ELAV protein during *Drosophila* melanogaster development. J. Neurobiol 22, 443–461. [PubMed: 1716300]

Sasamura T, Sasaki N, Miyashita F, Nakao S, Ishikawa HO, Ito M, Kitagawa M, Harigaya K, Spana E, Bilder D, et al. (2003). neurotic, a novel maternal neurogenic gene, encodes an O-fucosyltransferase that is essential for Notch-Delta interactions. Development 130, 4785–4795. [PubMed: 12917292]

Shao L, Moloney DJ, and Haltiwanger R (2003). Fringe modifies O-fucose on mouse Notch1 at epidermal growth factor-like repeats within the ligand-binding site and the Abruptex region. J. Biol. Chem 278, 7775–7782. [PubMed: 12486116]

Shi S, and Stanley P (2003). Protein O-fucosyltransferase 1 is an essential component of Notch signaling pathways. Proc. Natl. Acad. Sci. USA 100, 5234–5239. [PubMed: 12697902]

Shi S, Ge C, Luo Y, Hou X, Haltiwanger RS, and Stanley P (2007). The threonine that carries fucose, but not fucose, is required for Cripto to facilitate Nodal signaling. J. Biol. Chem 282, 20133–20141. [PubMed: 17504756]

Siebel C, and Lendahl U (2017). Notch Signaling in Development, Tissue Homeostasis, and Disease. Physiol. Rev 97, 1235–1294. [PubMed: 28794168]

Sprinzak D, Lakhanpal A, Lebon L, Santat LA, Fontes ME, Anderson GA, Garcia-Ojalvo J, and Elowitz MB (2010). Cis-interactions between Notch and Delta generate mutually exclusive signalling states. Nature 465, 86–90. [PubMed: 20418862]

Stanley P, and Okajima T (2010). Roles of glycosylation in Notch signaling. Curr. Top. Dev. Biol 92, 131–164. [PubMed: 20816394]

Takeuchi H, and Haltiwanger RS (2014). Significance of glycosylation in Notch signaling. Biochem. Biophys. Res. Commun 453, 235–242. [PubMed: 24909690]

Taylor P, Takeuchi H, Sheppard D, Chillakuri C, Lea SM, Haltiwanger RS, and Handford PA (2014). Fringe-mediated extension of O-linked fucose in the ligand-binding region of Notch1 increases binding to mammalian Notch ligands. Proc. Natl. Acad. Sci. USA 111, 7290–7295. [PubMed: 24803430]

Varshney S, and Stanley P (2018). Multiple roles for O-glycans in Notch signalling. FEBS Lett. 592, 3819–3834. [PubMed: 30207383]

Venken KJ, He Y, Hoskins RA, and Bellen HJ (2006). P[acman]: a BAC transgenic platform for targeted insertion of large DNA fragments in D. melanogaster. Science 314, 1747–1751. [PubMed: 17138868]

Venken KJ, Carlson JW, Schulze KL, Pan H, He Y, Spokony R, Wan KH, Koriabine M, de Jong PJ, White KP, et al. (2009). Versatile P[acman] BAC libraries for transgenesis studies in *Drosophila* melanogaster. Nat. Methods 6, 431–434. [PubMed: 19465919]

Wang Y, and Spellman MW (1998). Purification and characterization of a GDP-fucose:polypeptide fucosyltransferase from Chinese hamster ovary cells. J. Biol. Chem 273, 8112–8118. [PubMed: 9525914]

Wang Y, Shao L, Shi S, Harris RJ, Spellman MW, Stanley P, and Haltiwanger RS (2001). Modification of epidermal growth factor-like repeats with O-fucose. Molecular cloning and expression of a novel GDP-fucose protein O-fucosyltransferase. J. Biol. Chem 276, 40338–40345. [PubMed: 11524432]

Xu A, Lei L, and Irvine KD (2005). Regions of *Drosophila* Notch that contribute to ligand binding and the modulatory influence of Fringe. J. Biol. Chem 280, 30158–30165. [PubMed: 15994325]

Xu A, Haines N, Dlugosz M, Rana NA, Takeuchi H, Haltiwanger RS, and Irvine KD (2007). In vitro reconstitution of the modulation of *Drosophila* Notch-ligand binding by Fringe. J. Biol. Chem 282, 35153–35162. [PubMed: 17923477]

Yamamoto S, Charng WL, Rana NA, Kakuda S, Jaiswal M, Bayat V, Xiong B, Zhang K, Sandoval H, David G, et al. (2012). A mutation in EGF repeat-8 of Notch discriminates between Serrate/Jagged and Delta family ligands. Science 338, 1229–1232. [PubMed: 23197537]

Yang LT, Nichols JT, Yao C, Manilay JO, Robey EA, and Weinmaster G (2005). Fringe glycosyltransferases differentially modulate Notch1 proteolysis induced by Delta1 and Jagged1. Mol. Biol. Cell 16, 927–942. [PubMed: 15574878]

Zeng C, Younger-Shepherd S, Jan LY, and Jan YN (1998). Delta and Serrate are redundant Notch ligands required for asymmetric cell divisions within the *Drosophila* sensory organ lineage. Genes Dev. 12, 1086–1091. [PubMed: 9553038]

Zhang N, and Gridley T (1998). Defects in somite formation in lunatic fringe-deficient mice. Nature 394, 374–377. [PubMed: 9690472]

Highlights

- Fringe regulates fly Notch signaling by adding GlcNAc to *O*-fucose on Notch EGF8, −9, and −12
- *O*-Fucose monosaccharide on Notch EGF12 is essential for fly embryonic neurogenesis
- Fringe-modified EGF8, −9, and −12 promote Delta-Notch signaling in wing vein formation
- Fringe-modified EGF8 and −12 prevent *cis*-inhibition of Serrate by Notch *in vivo*

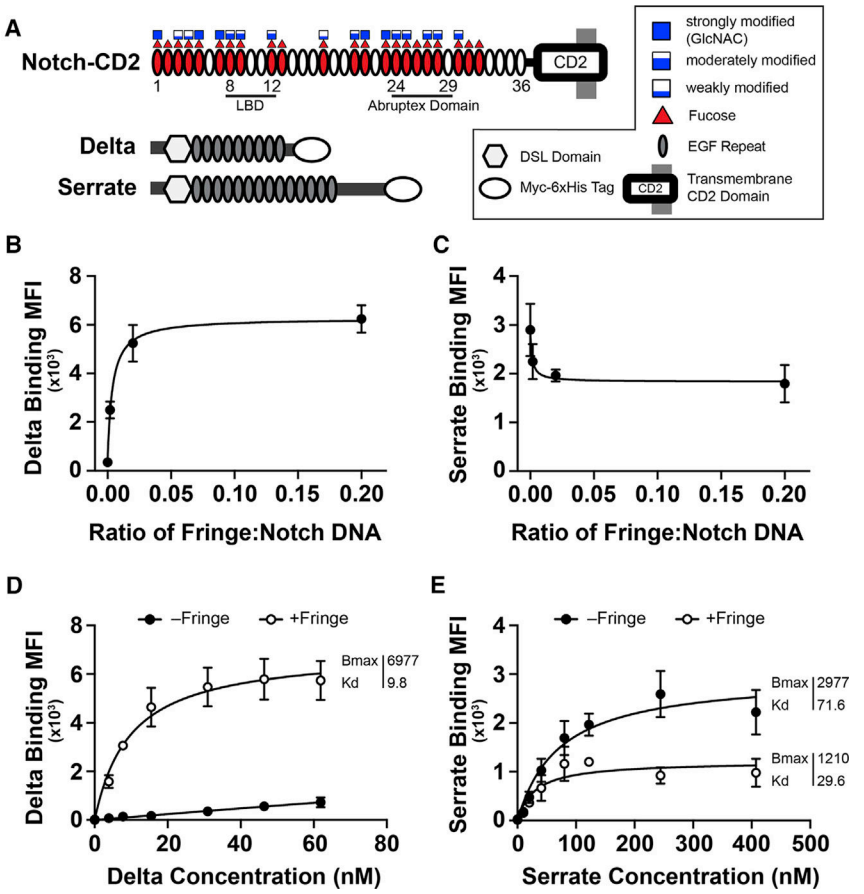

Figure 1. Fng Differentially Affects Notch Binding to Dl and Ser

(A) Schematic of proteins used in the cell-based ligand binding assay. Notch-CD2 (N-CD2) contains EGF repeats 1–36 from *Drosophila* Notch fused to a transmembrane CD2 protein. EGF repeats containing an *O*-fucose consensus sequence ($C^2X_{4–5}(S/T)C^3$) are in red. The presence of *O*-fucose on an EGF repeat is indicated by a red triangle and elongation by Fringe by a blue square based on previously published mass spectral analysis (Harvey et al., 2016). The extent of Fringe modification is indicated by the partially filled blue squares as shown in the key. The ligand-binding domain (LBD) and the *Abruptex* domain are also indicated. The extracellular domains of fly ligands Dl and Ser have C-terminal Myc-6xHis tags.

(B and C) Cell-based ligand binding assays of S2 cells co-transfected with N-CD2 and increasing amounts of Fng. Cells were incubated with (B) 15.5 nM Dl-Myc-6xHis or (C) 203.7 nM Ser-Myc-6xHis pre-clustered with phycoerythrin (PE)-conjugated anti-myc antibody, and binding was detected using flow cytometric analysis. Binding is represented as mean fluorescence intensity (MFI).

(D and E) Cell-based ligand binding assays of S2 cells co-transfected with N-CD2 and empty vector control (−Fringe) or an Fng expression vector (+Fringe; Fringe:Notch DNA ratio 1:1) incubated with varying amounts of (D) Dl-Myc-6xHis protein or (E) Ser-Myc-6xHis protein.

Maximum binding (Bmax) and the half-maximum ligand binding concentration (Kd) were estimated with Prism (GraphPad Software). Data points represent means ± SDs of three independent experiments.

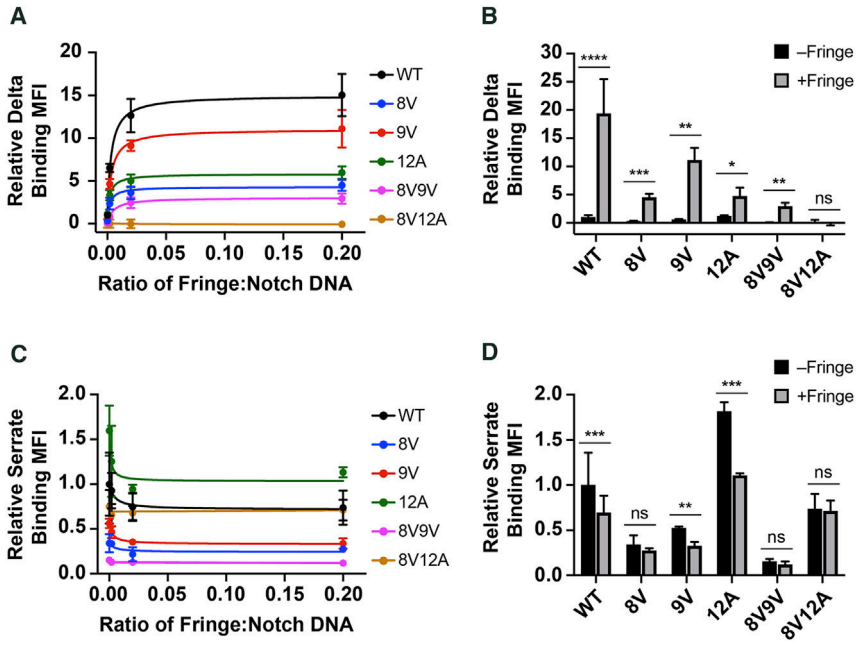

Figure 2. Fng Modulates Ligand Binding through *O*-fuc Sites on EGF8, EGF9, and EGF12

(A) Cell-based ligand-binding assays of S2 cells co-transfected with N-CD2 or certain *O*-fuc site N-CD2 mutants and increasing amounts of Fng. Cells were incubated with 15.5 nM Dl-Myc-6xHis pre-clustered with PE-conjugated anti-myc antibody labeling, and binding was detected by flow cytometric analysis.

(B) Cell-based ligand binding assays of S2 cells co-transfected with wild-type (WT) N-CD2 or *O*-fuc site N-CD2 mutants and empty vector control (−Fringe) or Fng (+Fringe; Fringe:Notch DNA ratio 0.2:1). Dl binding was detected as described in (A).

(C) Cell-based ligand binding assays of S2 cells co-transfected with N-CD2 or certain *O*-fuc site N-CD2 mutants and increasing amounts of Fng. Cells were incubated with 203.7 nM Ser-Myc-6xHis and ligand binding was detected by PE-conjugated anti-myc antibody labeling and flow cytometric analysis.

(D) Cell-based ligand-binding assays of S2 cells co-transfected with WT N-CD2 or *O*-fuc site N-CD2 mutants and empty vector control (−Fringe) or Fng (+Fringe; Fringe:Notch DNA ratio 0.2:1). Ser-Myc-6xHis binding was detected as described in (C).

Binding is represented as relative mean fluorescence intensity (MFI). Data points represent means ± SDs of three independent experiments. ns, not significant ($p > 0.05$), *$p < 0.05$, **$p < 0.01$, ***$p < 0.001$, ****$p < 0.0001$ (Student's t test).

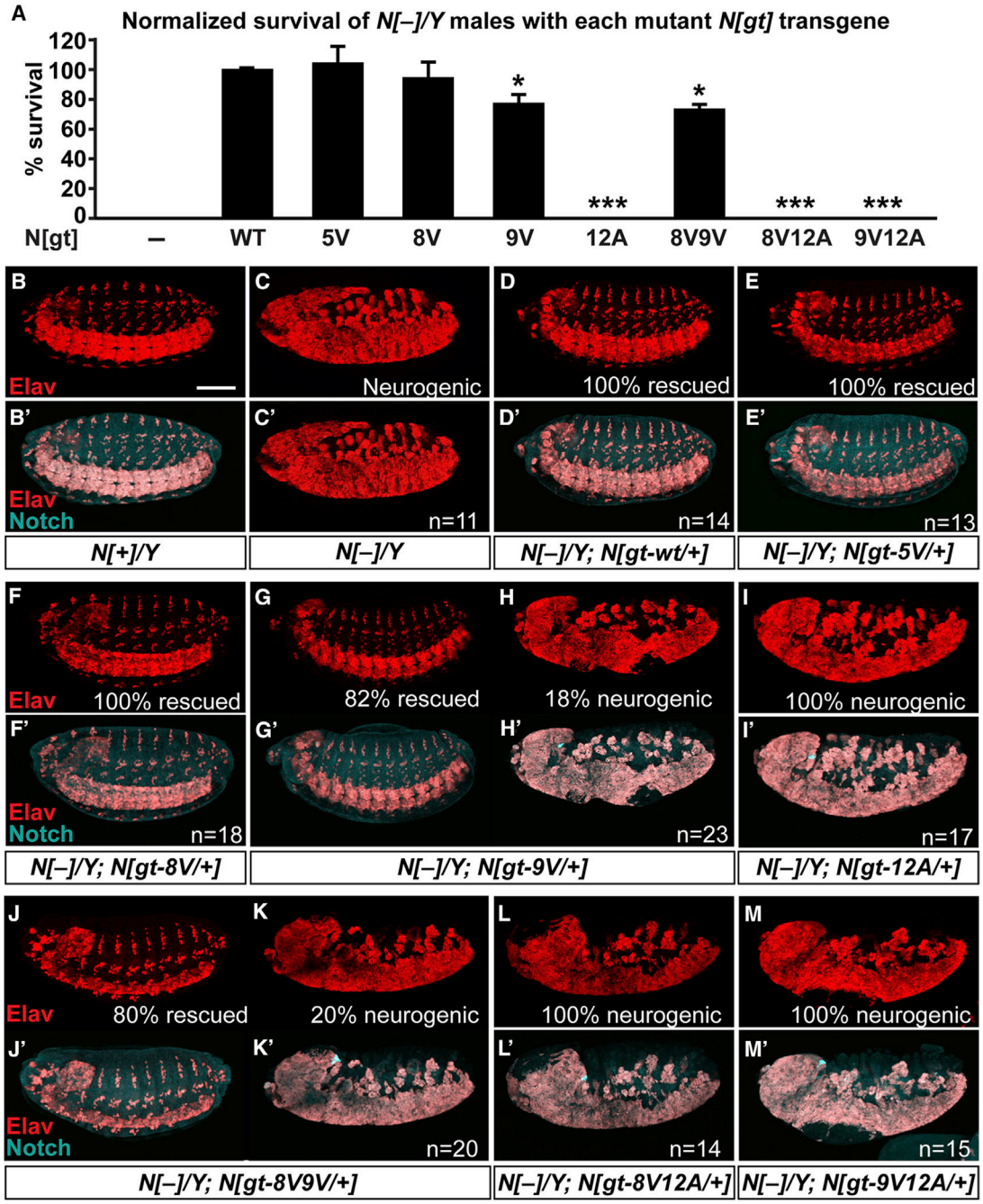

Figure 3. Mutation in the Notch EGF12 *O*-Fucosylation Site Abolishes Its Ability to Rescue Lethality and Neurogenic Phenotype in *Notch* Null Males

(A) Graph showing the survivability of *Notch* hemizygous males to adulthood in the presence of wild-type and mutant *Notch* transgenes. Data presented as means ± SDs, *p < 0.05, ***p < 0.001 (one-way ANOVA followed by Dunnett's post hoc test).

(B–M') ELAV (red) and Notch (magenta) staining in embryos. (B–M) show ELAV staining in *N[+]/Y* (B) and *N[−]/Y* embryos (C) or *N[−]/Y* embryos with one copy of wild-type (D) or mutant (E–M) Notch genomic transgenes, as shown in each panel. (B'–M') show ELAV/Notch double-staining for the same genotypes.

Scale bar in (B), 50 μm (applies to all of the panels). Note that the *N[−]/Y* embryo shown in (C') does not exhibit magenta staining for Notch, confirming that it is a null allele.

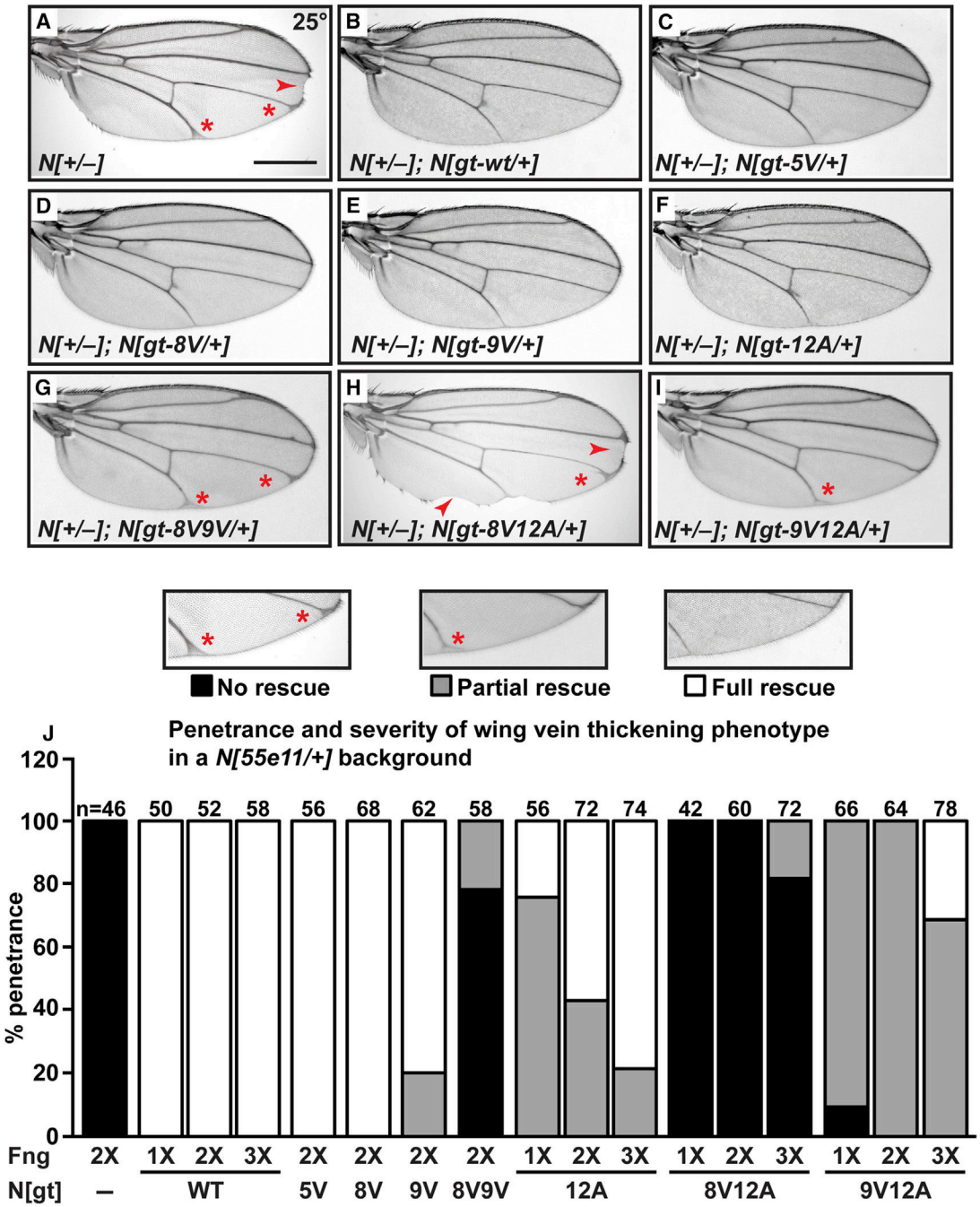

Figure 4. Wing Vein Thickening and Wing Margin Loss Phenotypes of *N[+/−]* Flies in the Absence or Presence of Wild-Type and Mutant *Notch* Genomic Transgenes

All of the animals were raised at 25°C.

(A) A wing from an *N[+/−]* fly showing wing vein thickening (red asterisk) and wing margin loss (red arrowhead) phenotypes. Scale bar, 0.5 mm (applies to all of the panels).

(B–I) *N[+/−]* wings with one copy of wild-type (B) or mutant (C–I) *Notch* genomic transgenes, as shown in each panel.

(J) Percentages of each class of wing vein-thickening phenotype (no rescue, partial rescue, and full rescue) in (A)–(I) and upon removing (1X) or adding (3X) one copy of *fng* in some

genetic backgrounds. To add or remove one copy of *fng, PBac{CH321–87O20}VK37* and fng^{L73} strains, respectively, were used.

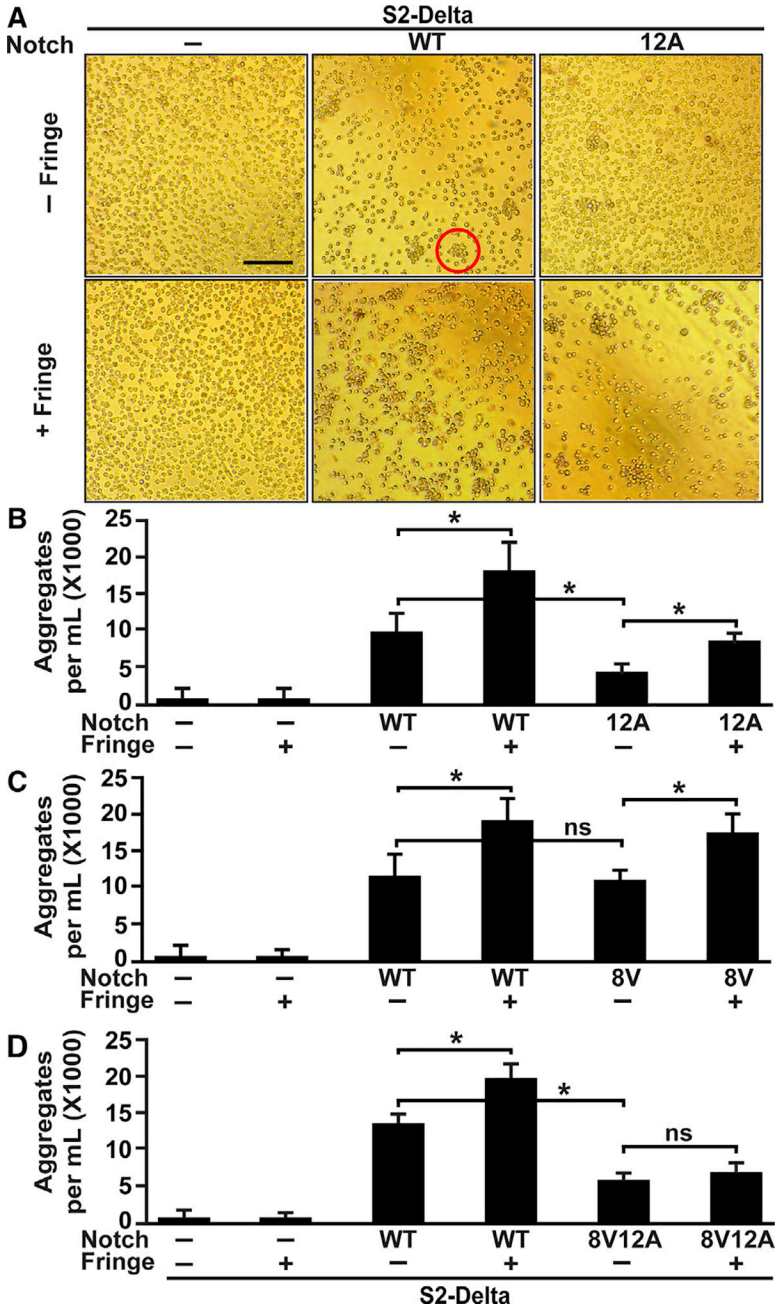

Figure 5. Cell-Based Aggregation Assays Indicate Decreased Notch-Dl Binding upon the Loss of Fucosylation at EGF12 and Abolished Fng Effect on Notch-Dl Binding upon the Loss of the GlcNAc-fuc-*O* Glycans at Both EGF8 and EGF12

(A) Representative images of aggregation between the indicated cell types in the absence (top panel) and presence of Fng (bottom panel). The red circle indicates a representative aggregate in one of the panels. Scale bar, 100 μm (applies to all of the panels).

(B) Graphs showing the quantification of the number of cell aggregates between the indicated cell types after 5 min.

(C) Graphs showing the quantification of the number of cell aggregates between the indicated cell types after 5 minutes.

(D) Graphs showing the quantification of the number of cell aggregates between the indicated cell types after 5 min.

Data presented as means ± SDs. ns, not significant ($p > 0.05$), *$p < 0.05$ (one-way ANOVA followed by Dunnett's post hoc test).

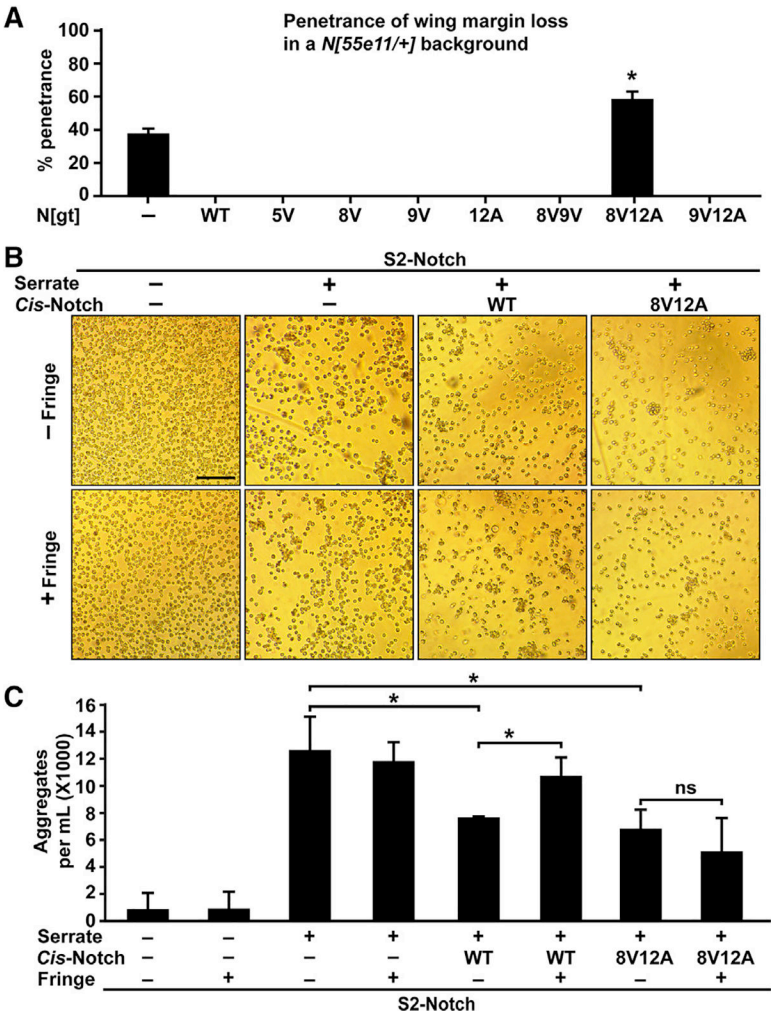

Figure 6. *N[gt]* with *O*-Fuc Mutations in Both EGF8 and EGF12 Shows a Dominant Negative Wing Margin Loss Phenotype *In Vivo* and Enhances *cis*-Binding with Ser in an S2 Cell-Based Aggregation Assay

(A) Graph showing the penetrance of the wing margin loss phenotype in an *N[+/−]* background in the absence and presence of wild-type (WT) and mutated *Notch* transgenes.

(B) Representative images of aggregation between the indicated cell types in the absence (top panel) and presence of Fng (bottom panel). Scale bar, 100 μm (applies to all of the panels).

(C) Graph showing the quantification of the number of cell aggregates between the indicated cell types after 5 min. WT, WT *Notch* cDNA, 8V12A, *Notch* cDNA with mutated *O*-fucosylation sites at both EGF8 and EGF12.

Data presented as means ± SDs. ns, not significant ($p > 0.05$), *$p < 0.05$ (one-way ANOVA followed by Dunnett's post hoc test).

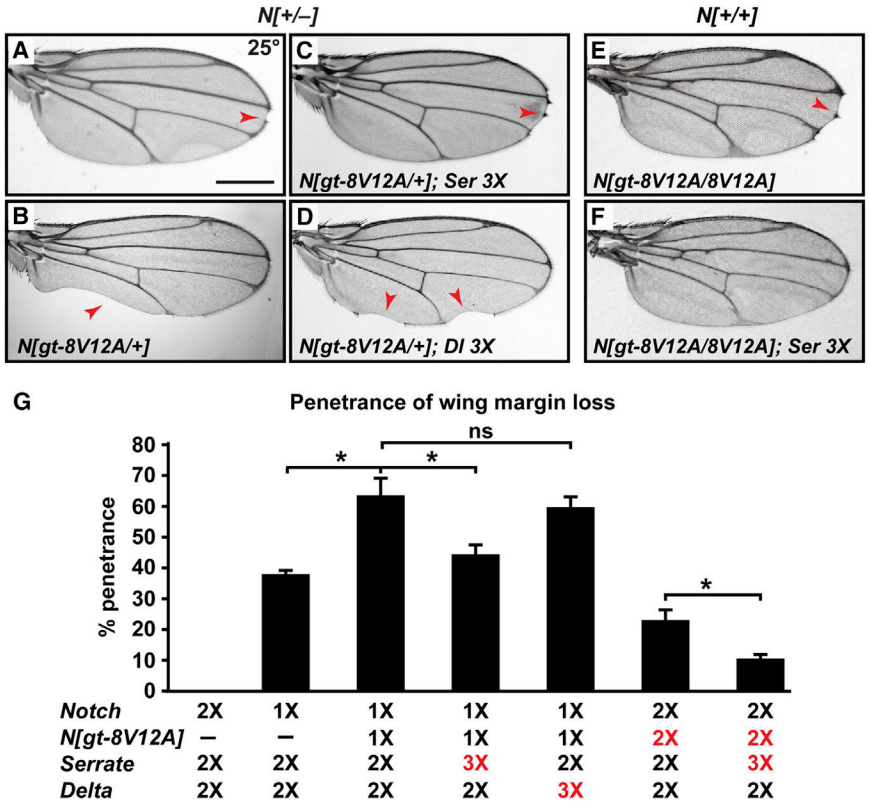

Figure 7. Increasing *Ser* Gene Dosage Suppresses the Dominant Negative Wing Margin Loss Phenotype Exhibited by *N[gt-8V12A]*

(A–D) Wings from *N[+/−]* alone (A) and *N[+/−]* with one copy of *N[gt-8V12A]* (B–D). (C) has an extra copy of *Ser*, and (D) has an extra copy of *Dl*.

(E–F) *N[+/+]* wings with two copies of *N[gt-8V12A]* only (E) or in combination with an extra copy of *Ser* (F). Red arrowheads show wing margin loss. Animals were raised at 25°C. Scale bar in (A), 0.5 mm (applies to all of the panels).

(G) Graph showing the penetrance of wing margin loss in the indicated genotypes. Data presented as means ± SDs. ns, not significant ($p > 0.05$), *$p < 0.05$ (one-way ANOVA followed by Dunnett's post hoc test).

KEY RESOURCES TABLE

REAGENT or RESOURCE	SOURCE	IDENTIFIER
Antibodies		
mouse anti-CD2 (OX-34 clone) (1:100)	Bio-Rad	Product Code MCA154GA; RRID: AB_566608
Mouse anti-Notch (F461.3B)	DSHB	RRID: AB_528409
Rabbit anti-V5	Sigma Aldrich	RRID: AB_261889; Product Number V8137
Alexa Fluor680 rabbit anti-mouse	Invitrogen	Cat # A-21065; RRID: AB_2535728
HRP-conjugated goat anti-mouse	Jackson ImmunoResearch Lab	Code 115–035–044; RRID: AB_2338503
PE-conjugated goat anti-mouse	Life Technologies	Cat # P-852; RRID: AB_2539848
PE-conjugated mouse anti-myc (9E10 clone)	R&D systems	Cat # IC3696P
IRDye700 goat anti-rabbit	Rockland Immunochemicals	Cat # 611–130–002; RRID: AB_1660969
Goat anti-rat Cy3-conjugated 1:500	Jackson ImmunoResearch Lab	RRID: AB_2338240
Goat anti-mouse Alexa Fluor-488	Jackson ImmunoResearch Lab	RRID: AB_2338840
Mouse anti-Notch (C458.2H), 1:100	DSHB	RRID: AB_528408
Rat-Elav-7E8A10 anti-Elav, 1:200	DSHB	RRID: AB_528218
Chemicals, Peptides, and Recombinant Proteins		
Blasticidin	Invitrogen	Cat# R210–01
methotrexate	Sigma-Aldrich	M9929, CAS: 0133073731
FuGENE HD	Promega	Cat # E2311
Hygromycin B	Invitrogen	Cat# 10687010
Critical Commercial Assays		
Calcium Phosphate Transfection Kit	Invitrogen	Cat # K2780–01
QuikChange II XL Site-Directed Mutagenesis Kit	Agilent Technologies	Cat # 200522
Effectene Reagent	QIAGEN	Cat # 301425
Experimental Models: Cell Lines		
S2 cells	Invitrogen	Cat # R69007
S2-Dl-Myc-6xHis stable cell line	This study	N/A
S2-Ser-Myc-6xHis stable cell line	This study	N/A
S2-N stable cell lines	Drosophila Genomics Resource Center (DGRC)	Stock No:154 FBtc0000154
S2-Dl stable cell lines	DGRC	Stock No: 152
S2-Ser^{Tom} stable cells	Fleming et al., 2013	FBtc0000152
Experimental Models: Organisms/Strains		
y w	Bloomington Drosophila Stock Center (BDSC)	BDSC#6598
w; noc^{Sco}/CyO; TM3, Sb^{1}/TM6, Tb^{1}	Lee et al., 2013	N/A
y w, N^{55e11}/FM7c, B^{1}	Leonardi et al., 2011	N/A

REAGENT or RESOURCE	SOURCE	IDENTIFIER
y w, N^{54l9} FRT19A/FM7C, B^{1}	Leonardi et al., 2011	N/A
y w Ubx-FLP Tub-GAL80 FRT19A; Act-GAL4 UAS-GFP^{nls}/CyO, y^{+}	Leonardi et al., 2011	N/A
y w; PBac{$N^{gt\text{-}wt}$}VK22	Leonardi et al., 2011	N/A
y w; PBac{$N^{gt\text{-}5V}$}VK22	This study	N/A
y w; PBac{$N^{gt\text{-}8V}$}VK22	This study	N/A
y w; PBac{$N^{gt\text{-}9V}$}VK22	This study	N/A
y w; PBac{N^{gt12AV}}VK22	This study	N/A
y w; PBac{$N^{gt\text{-}8V9V}$}VK22	This study	N/A
y w; PBac{$N^{gt\text{-}8V12A}$}VK22	This study	N/A
y w; PBac{$N^{gt\text{-}9V12A}$}VK22	This study	N/A
y w; PBac{$N^{gt\text{-}9S}$}VK22	This study	N/A
y w; PBac{$N^{gt\text{-}12T}$}VK22	This study	N/A
y w; PBac{$Ser^{gt\text{-}wt}$}VK31	This study	N/A
y w; P{$Dl^{gt\text{-}wt}$}attP2	LeBon et al., 2014	N/A
fng^{L73}/TM3,Sb^{1}	Correia et al., 2003	N/A
PBac{*CH321–87O20*}VK37	Genetivision	Stock ID#P12-A6
Oligonucleotides		
Primers used for Site-directed mutagenesis of N-CD2 and Fringe for binding assays are listed in Supplementary table (Table S1)	This study Table S1	N/A
Primer pair for generating EGF8TV for cell-based aggregation assay 5′-CGGAGCCGTCTGTACAAACACTCACGGATCG-3′ and 5′-TGTACAGACGGCTCCGTTCTGGCACACCGG-3′.	This study	N/A
Primer pair for generating EGF12SA for cell-based aggregation assay 5′-CGAGGGAGCTTGCCTGGATGATCCGG-3′ and 5′-CAGGCAAGCTCCCTCGTTCTGGCATGG-3′	This study	N/A
Recombinant DNA		
pMT-Notch	DGRC	Stock number 1022
pMT-Ser	Okajima et al., 2003	Ken Irvine lab
pMT-fng	Brückner et al., 2000	Cohen lab
BAC clone attB-P[acman]-CmR-CH321–69C08	Venken et al., 2009	N/A
pMT-N-CD2	Yamamoto et al., 2012	From Shinya Yamamoto
pMT-V5His	Thermo Fisher	Cat# V412020
pMT-Fng-V5His	This study	N/A
EGFP-N1	Clontech	Cat #6085–1
pMT-GFP	This study	N/A
pMT-Dl-Myc-6xHis	This study	N/A
pMT-Ser-Myc-6xHis	This study	N/A
pMT-Dl-AP	Okajima et al., 2003	Ken Irvine lab
pMT-Ser-AP	Okajima et al., 2003	Ken Irvine lab
Software and Algorithms		

REAGENT or RESOURCE	SOURCE	IDENTIFIER
FlowJo software	FlowJo	https://www.flowjo.com/solutions/flowjo/downloads
Amira5.2.2	Thermo Scientific	
ImgaeJ1.47	NIH	https://imagej.nih.gov/ij/
Prism 6	Graphpad	https://graphpad-prism.software.informer.com/6.0/
Adobe Illustrator CS5.1	Adobe	https://www.adobe.com/products/illustrator.html
Adobe Photoshop CS5	Adobe	https://www.adobe.com/products/photoshop.html